THE ASTROPHYSICAL JOURNAL, 588:975–991, 2003 May 10

THE CRUSTAL RIGIDITY OF A NEUTRON STAR AND IMPLICATIONS FOR PSR B1828−11 AND OTHER PRECESSION CANDIDATES

CURT CUTLER
Max-Planck-Institut für Gravitationsphysik Golm bei Potsdam, Germany; cutler@aei.mpg.de

GREG USHOMIRSKY
California Institute of Technology, Pasadena, CA; gregus@tapir.caltech.edu

AND

BENNETT LINK
Montana State University, Bozeman, MT; blink@dante.physics.montana.edu
Received 2002 October 8; accepted 2002 December 24

ABSTRACT

Like the Earth, a neutron star (NS) can undergo torque-free precession because some piece ΔI_d of its inertia tensor remains tied to the crust's principal axes, as opposed to following the crust's angular velocity vector. The (body frame) precession frequency ν_p is $\nu_s \Delta I_d / I_C$, where ν_s is the NS's spin frequency and I_C is the moment of inertia associated with the crustal nuclei, plus any component of the star tightly coupled to the crust over a timescale less than the spin period. For a spinning NS with a relaxed crust, $\Delta I_d = b \Delta I_\Omega$, where ΔI_Ω is the rotational oblateness of a fluid star rotating at spin frequency Ω and b is the NS's *rigidity parameter*. A previous estimate of b by Baym & Pines gives $b \sim 10^{-5}$ for typical NS parameters. Here we calculate the rigidity parameter b and show that it is ∼40 times smaller than the Baym-Pines estimate. We apply this result to PSR B1828−11, an isolated pulsar whose correlated timing residuals and pulse shape variations provide strong evidence for precession with a 511 day period. We show that this precession period is ∼250 times shorter than one would expect, assuming that (1) the crust is relaxed (except for the stresses induced by the precession itself) and (2) the NS possesses no other source of stress that would deform its figure (e.g., a strong magnetic field). We conclude that the crust must be under significant stress to explain the precession period of PSR B1828−11; such stress arises naturally as the star spins down. Assuming that crustal shear stresses do set the precession period, the star's reference angular velocity (roughly, the spin at which the crust is most relaxed) is ≈40 Hz (i.e., $\approx\sqrt{250}$ times faster than today's spin), and the weighted average of the crust's present spin-down strain is $\bar{\sigma}^{\rm sd}_{\rm ave} \simeq 5 \times 10^{-5}$. We briefly describe the implications of our improved b calculation for other precession candidates.

Subject headings: dense matter — pulsars: individual (PSR 1828−11) — stars: neutron — stars: rotation

1. INTRODUCTION

Stairs, Lyne, & Shemar (2000) recently reported strong evidence for free precession in the radio pulsar PSR B1828−11. This pulsar has period $P_s = 0.405$ s, $\dot{P}_s = 6.00 \times 10^{-14}$, a characteristic age of $\tau_c = 0.11$ Myr, and an inferred B field of 5.0×10^{12} G. Timing residuals for PSR B1828−11 show strong periodic modulation, with periods of 511 and 256 days. A 1009 day periodicity is also claimed, but with lower confidence.

The 511 and 256 day timing residuals are matched by periodic modulations of the pulse shape, which strongly supports the interpretation that the modulations are due to neutron star (NS) precession, with a wobble amplitude of ∼3°. In the model of Link & Epstein (2001), free precession sets the 511 day timescale, while coupling of the precession to the external electromagnetic torque produces variations in the NS's spin-down rate that give the main contribution to the timing residuals (due to the changing angle between the NS's magnetic dipole axis and spin direction) and produce a harmonic at 256 days.

While periodic or quasi-periodic timing residuals have been observed in several other isolated pulsars (including B1642−03, the Crab, and Vela) and tentatively interpreted as evidence for torque-free precession (see Jones & Andersson 2001 for a review), PSR B1828−11 certainly represents the most convincing case for free precession in a NS. This pulsar has prompted us to reexamine theoretical estimates of a NS's (body frame) free-precession frequency, ν_p. If the crust is essentially relaxed, the body frame precession period is $P_p = (\nu_s)^{-1} I_C / \Delta I_d$, where ν_s is the spin frequency, I_C is the moment of inertia of the crust (plus any portion of the NS strongly coupled to the crust on a timescale $< \nu_s^{-1}$), and ΔI_d is the residual oblateness the NS *would* have if it were spun down to zero frequency without the crust breaking or otherwise relaxing (Pines & Shaham 1972a, 1972b; Munk & MacDonald 1960). For a crust that is relaxed at its current spin rate, we can write

$$\Delta I_d = b \Delta I_\Omega \,, \tag{1}$$

where ΔI_Ω is the piece of the NS's inertia tensor due to its spin (i.e., to centrifugal force), approximately given by

$$\Delta I_\Omega \approx 0.3 I_0 (\nu_s / \mathrm{kHz})^2 \tag{2}$$

(Jones 2000), where I_0 is the total moment of inertia for the star when nonrotating. The coefficient b in equation (1) is sometimes called the NS's "rigidity parameter" (Jones & Andersson 2000).

This paper is concerned with an accurate calculation of b. For the case of a star with constant density and constant shear modulus, the result is $b = (57/10)\mu V / |E_g|$, where μ

is the shear modulus, V is the star's volume, and $E_g = -\frac{3}{5}GM^2/R$ is star's gravitational binding energy (Love 1944, p. 259). As a estimate for a NS with a liquid core, Baym & Pines (1971) took

$$b \approx \frac{57}{10}|E_g|^{-1}\int \mu\, dV \sim 10^{-5}\,, \tag{3}$$

for a 1.4 $M_\odot$ NS. The Baym-Pines estimate for b, equation (3), has been routinely adopted in the NS precession literature.

In this paper, we mainly do two things. First, we calculate b for realistic NS structure—a solid crust afloat on a liquid core. We solve for the strain field that develops as the NS spins down and find that b is smaller than that found by Baym & Pines (1971) by a factor of $\sim$40. A partial explanation of why equation (3) yields so large an overestimate is given in the appendices.

Second, we use our improved b-value to show that PSR B1828$-$11 is precessing $\sim$250 times faster than one would expect, assuming that its crust is nearly relaxed. Under the hypothesis that crust rigidity is the dominant source of the deformation bulge ΔI_d (and that the observed modulations are indeed due to precession), we conclude that the crust of PSR B1828$-$11 is *not* currently relaxed and that its reference spin $\nu_{s,\mathrm{ref}}$ (roughly, the spin at which the crust is most relaxed) is approximately 40 Hz, i.e., $\approx\sqrt{250}$ times higher than the current spin. (In this sense, the precession of PSR B1828$-$11 is different from the Chandler wobble of the Earth since the Earth *is* almost relaxed.)

As we explain in § 5, the current strain tensor in the crust σ_{ab} can be written as the sum of "spin-down" (sd) and "reference" (ref) pieces: $\sigma_{\mathrm{ab}} = \sigma^{\mathrm{sd}}_{\mathrm{ab}} + \sigma^{\mathrm{ref}}_{\mathrm{ab}}$. The $\sigma^{\mathrm{ref}}_{\mathrm{ab}}$ piece is basically the strain that would exist in the crust, even if it were spinning at $\nu_{s,\mathrm{ref}}$; $\sigma^{\mathrm{ref}}_{\mathrm{ab}}$ depends on the detailed history of local crust quakes/relaxations and is thus unknown. The spin-down strain $\sigma^{\mathrm{sd}}_{\mathrm{ab}}$ is the strain induced as the NS spins down from ν_{ref} to its current value ν_s. For PSR B1828$-$11, we show that its weighted average is $\bar{\sigma}^{\mathrm{sd}}_{\mathrm{ave}} \sim 5\times10^{-5}$.

Although $\sigma^{\mathrm{ref}}_{\mathrm{ab}}$ is unknown, it seems likely to us that the full strain is larger, on average, than the spin-down strain. [This is because the full strain $\bar{\sigma} \equiv (0.5\sigma_{\mathrm{ab}}\sigma^{\mathrm{ab}})^{1/2}$ contains contributions from all harmonics, while the spin-down strain is entirely in the Y_{20} harmonic.] *If* this is true, then the NS's crustal breaking strain $\bar{\sigma}_{\max}$ must be larger than the average spin-down value: $\bar{\sigma}_{\max} > \bar{\sigma}^{\mathrm{sd}}_{\mathrm{ave}} \sim 5\times10^{-5}$. Although $\bar{\sigma}_{\max}$ is poorly constrained, both empirically and theoretically, a value this large seems quite reasonable: the usual assumption has been that $\bar{\sigma}_{\max}$ for NS crusts is somewhere in the range 10^{-5} to 10^{-1}. (Unlike the crust's shear modulus, which can be estimated from simple energetics, the breaking strain $\bar{\sigma}_{\max}$ depends on the type, density, and propagation of dislocations in the lattice, which are highly uncertain.)

If significant pinning of superfluid vortex lines to the nuclear lattice or to flux tubes in the core occurs, the precession frequency is not set by the material properties of the crust (Shaham 1977). In this situation, the pinned superfluid behaves effectively as a large ΔI_d, equal to the moment of inertia I_p of the pinned superfluid. For example, if the entire crust superfluid pins to the solid, I_p is $\sim 0.01 I_0 \sim I_C$. The (body frame) precession frequency should then be of the order of the spin frequency (or at most $\sim$100 times slower, if the crust-core coupling is much larger than usually presumed, so $I_C \sim I_0$). Instead, in PSR B1828$-$11 and the other precession candidates reviewed in § 6, the precession frequency is $\sim$6–8 orders of magnitude *lower* than the spin frequency. Thus, claims for long-period NS precession appeared at first to conflict with one explanation for large pulsar glitches, wherein superfluid vortices do pin to crustal nuclei and large glitches represent large-scale unpinning events (see, e.g., Anderson & Itoh 1975). This conflict was recently resolved by Link & Cutler (2001), who showed that, in PSR B1828$-$11 and other precession candidates, the precessional motion itself exerts Magnus forces on the vortices that are $\gtrsim$100 times larger than the Magnus forces responsible for giant glitches. (The fact that sufficiently large, precession-induced Magnus forces would unpin superfluid vortices had been noted previously by Shaham 1986.) That is, in all likelihood the precessional motion itself immediately unpins the superfluid vortices and keeps them unpinned. Accordingly, in this paper, we set $I_p = 0$. (Of course, pinning can persist in precessing stars if the wobble angle is sufficiently small.)

This paper is concerned with whether crustal stresses alone can give a NS precession period of the order of a year (for spin rates of a few Hz), but we mention that magnetic field stresses can also give a precession period of this order *if the core is a type II superconductor*, as shown recently by Wasserman (2003), in an extension of work by Mestel and collaborators (Mestel & Takhar 1972; Mestel et al. 1981; Nittmann & Wood 1981; see all of Spitzer 1958).

The plan of this paper is as follows. In § 2 we review the dynamics of NS precession, partly to establish notation. In § 3 we present our formalism for calculating the rigidity parameter b for a NS. In § 4 we present the results of this calculation: the value of b and the corresponding crustal stresses. Knowing b allows us to estimate the precession frequency of a NS with a relaxed crust. In § 5 we extend this result to a NS with a substantially strained crust. We apply these results to PSR B1828$-$11 in § 6, where we show that the observed precession frequency is $\sim$250 times higher than would be predicted for a relaxed crust. We calculate the spin-down strain levels that must exist today in the crust of PSR B1828$-$11, assuming that crustal shear stresses are indeed responsible for the observed precession frequency.

In § 7 we briefly discuss the implications of our work for some other NSs that show evidence for precession (the Crab, Vela, PSR B1642$-$03, PSR 2217+47, PSR B0959$-$54, and the possible remnant in SN 1987A). Our conclusions are summarized in § 8.

The appendices represent our attempts to check and understand our results for b—in particular, to understand why the Baym-Pines estimate is so much larger than the value we obtain. In Appendix A we represent ΔI_d as an integral over crustal shear stresses. The result for b we obtain in this way is consistent with our result in § 4 and gives more insight into how different stress components and different layers in the crust contribute to the final answer. In Appendix B we treat a case in which b can be obtained analytically—that of a uniform-density, incompressible star with a thin crust of constant shear modulus afloat on a liquid core. For this case, we show the actual b is $\simeq$5 times smaller than the Baym-Pines estimate, equation (3). In the realistic NS case, b is decreased by additional factor of $\sim$8 because the contributions to ΔI_d from the different stress components and from different layers in the crust tend to cancel each

other much more nearly than in the case of a thin, *uniform* crust.

2. MODEL AND RESULTS

Here we derive the basic equations describing the precession of a NS. In this section, and in §§ 3–6, we assume that the only sources of nonsphericity in the NS are centrifugal force and crustal shear stresses.

We idealize the precessing NS as having two components: C (for crust) and F (for fluid), having angular velocities Ω^a_C and Ω^a_F, respectively. Ω^a_C and Ω^a_F have the same magnitude Ω, but different directions. The C piece includes the crustal nuclei but may also include some component of the fluid that is coupled to the crust sufficiently strongly that it effectively corotates with the crust over timescales shorter than the rotation period $2\pi\Omega^{-1}$. The F piece is that portion of the fluid that is essentially decoupled from the crustal nuclei on this timescale; conservation of vorticity then implies that the fluid angular velocity Ω^a_F remains fixed and so is aligned with the NS's total angular momentum J^a:

$$\Omega^a_F = \Omega \hat{J}^a \ , \tag{4}$$

where $\hat{J}^a$ is the unit vector along J^a. The angular velocity of the crustal nuclei is $\Omega^a_C = \Omega\hat{\Omega}^a_C$, where $\hat{\Omega}^a_C$ is a unit vector.

We write the star's inertia tensor as

$$I_{\rm ab} = I_{F,\rm ab} + I_{C,\rm ab} \ , \tag{5}$$

where $I_{F,\rm ab}$ and $I_{C,\rm ab}$ are the contributions from the fluid interior and the solid crust, respectively. Following (and somewhat extending) Pines & Shaham (1972a, 1972b), we approximate each contribution as the sum of a spherical piece, plus a centrifugal bulge that follows that component's angular velocity, plus a deformation bulge (sustained by crustal rigidity) that follows some principal crustal axis $\hat{n}^a_d$:

$$\begin{aligned} I_{F,\rm ab} &= I_{F,0} g_{\rm ab} + \Delta I_{F,\Omega}\left(\hat{J}^a\hat{J}^b - \tfrac{1}{3} g_{\rm ab}\right) \\ &\quad + \Delta I_{F,d}\left(\hat{n}^a_d\hat{n}^b_d - \tfrac{1}{3} g_{\rm ab}\right) \ , \end{aligned} \tag{6}$$

$$\begin{aligned} I_{C,\rm ab} &= I_{C,0} g_{\rm ab} + \Delta I_{C,\Omega}\left(\hat{\Omega}^a_C\hat{\Omega}^b_C - \tfrac{1}{3} g_{\rm ab}\right) \\ &\quad + \Delta I_{C,d}\left(\hat{n}^a_d\hat{n}^b_d - \tfrac{1}{3} g_{\rm ab}\right) \ , \end{aligned} \tag{7}$$

where $g_{\rm ab}$ is the flat 3-metric [1, 1, 1]. The sum $\Delta I_d \equiv \Delta I_{C,d} + \Delta I_{F,d}$ we call the NS's *deformation bulge*; it is the nonsphericity the body would retain if it were slowed down to zero angular velocity, without the crust breaking or otherwise relaxing. Although ΔI_d is ultimately due to crustal shear stresses, the term $\Delta I_{F,d}$ is nonzero (even in the absence of pinning) because the crust exerts force on the fluid, both gravitationally and via pressure.

For a fully relaxed, rotating crust, we expect $\Delta I_d \propto \Delta I_\Omega$, where $\Delta I_\Omega \equiv \Delta I_{F,\Omega} + \Delta I_{C,\Omega}$ is the centrifugal piece of the entire star's inertia tensor and the coefficient of proportionality $b \equiv \Delta I_d/\Delta I_\Omega$ is the rigidity parameter. For a physical interpretation of b, let us take the Earth as an example. The Earth's crust is essentially relaxed. If we could slow the Earth down to zero angular velocity without cracking its crust, it would not settle directly into a spherical shape, but rather would remain somewhat oblate. This is because the Earth's relaxed, zero-strain shape is oblate, and after centrifugal forces are removed, the stresses that build up in the crust will tend to push it back toward that relaxed shape. In fact, for the Earth, $b \approx 0.7$ (Munk & MacDonald 1960, p. 40), so stopping the Earth from spinning would reduce its oblateness by only ~30%. For a NS, as we will see, $b \sim 2 \times 10^{-7}$, so halting a NS's rotation would decrease its oblateness by a factor of five million. The quantity b is so small for a NS because the gravitational energy density far exceeds the crust's shear modulus.

The total angular momentum J^a of fluid plus crust is

$$J_a = \Omega\left(I_{F,\rm ab}\hat{J}^b + I_{C,\rm ab}\hat{\Omega}^b_C\right) \ . \tag{8}$$

Note from equations (7) and (8) that $\hat{\Omega}^a_C$, $\hat{n}^a_d$, and $\hat{J}^a$ are all coplanar. Let J^a lie along the z-axis, and let $\hat{\Omega}^a_C$ and $\hat{n}^a$ lie, at some instant, in the (x, z)-plane, as illustrated in Figure 1. The angle between the crust's symmetry axis and angular velocity is θ. The angle between the angular velocity and the angular momentum is $\tilde{\theta}$. These angles are constants of the motion and satisfy

$$\hat{n}^a_d = \cos\theta\hat{z}^a - \sin\theta\hat{x}^a \ , \tag{9}$$

$$\hat{\Omega}^a_C = \cos\tilde{\theta}\hat{z}^a + \sin\tilde{\theta}\hat{x}^a \ . \tag{10}$$

From equations (9) and (10), we have, up to third-order terms in θ and $\tilde{\theta}$,

$$\Omega^a_C = \Omega\left(1 + \frac{\tilde{\theta}}{\theta} - \frac{1}{2}\theta^2 - \frac{1}{2}\tilde{\theta}\theta\right)\hat{J}^a - \frac{\tilde{\theta}}{\theta}\Omega\hat{n}^a_d \ . \tag{11}$$

From equation (11), we see that the precession is a

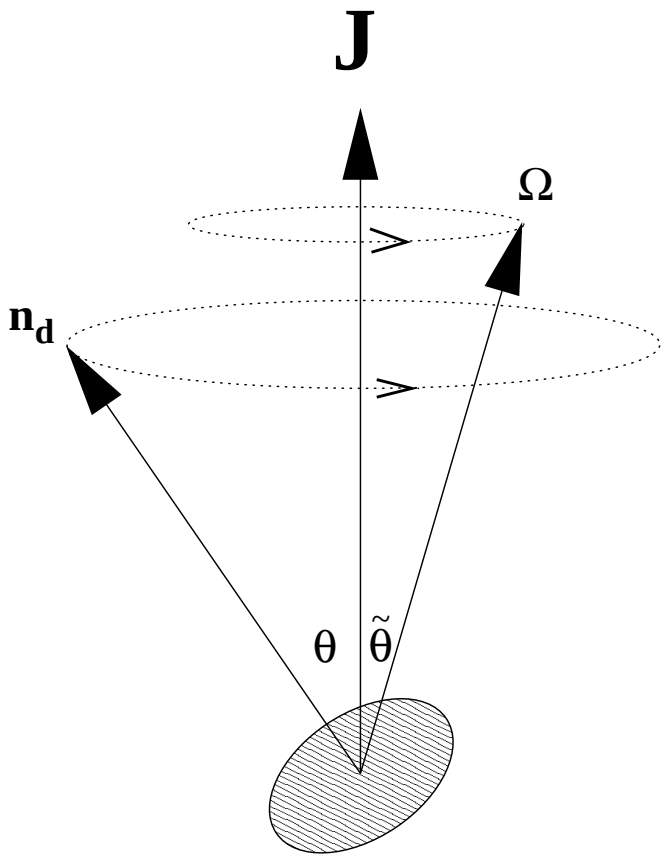

FIG. 1.—Definitions of the angles θ and $\tilde{\theta}$ in relation to the angular momentum vector J^a, the body axis $\hat{n}^a_d$, and the spin axis $\hat{\Omega}^a$.

superposition of two motions: $\hat{\boldsymbol{n}}_d^a$ precesses around $\hat{\boldsymbol{J}}^a$ with (inertial frame) precession frequency $\dot{\phi} = \Omega(1 + \tilde{\theta}/\theta)$, up to second-order terms in θ and $\tilde{\theta}$. Likewise, the coefficient of $\hat{\boldsymbol{n}}_d^a$ in equation (11) gives the body frame precession frequency: $\Omega_p = \Omega(\tilde{\theta}/\theta)$. For $\Omega > 0$ and $\Delta I_d > 0$, an observer situated above the pole $\hat{\boldsymbol{n}}_d^a$ and fixed in the body frame sees the angular velocity $\hat{\boldsymbol{\Omega}}^a$ circle around $\hat{\boldsymbol{n}}_d^a$ in the counterclockwise direction. The ratio $\tilde{\theta}/\theta$ is obtained directly by taking the x-component of equation (8); the result is

$$\tilde{\theta}/\theta = \frac{\Delta I_d}{I_{C,0} + (2/3)\Delta I_{C,\Omega} - (1/3)\Delta I_{C,d}} , \tag{12}$$

where $\Delta I_d \equiv \Delta I_{C,d} + \Delta I_{F,d}$. Since $\Delta I_{C,\Omega}$ and $\Delta I_{C,d}$ are tiny compared to $I_{C,0}$, we now ignore those terms and drop the subscript "0" from I_C. The (body frame) precession period P_p is thus

$$P_p = P_s \frac{I_C}{\Delta I_d} . \tag{13}$$

Since the pulsar's magnetic dipole moment and emission region are presumably fixed with respect to the crust, the angle between the dipole direction and $\hat{\boldsymbol{J}}^a$ varies on the timescale P_p; i.e., the body frame precession period P_p is the modulation period for the pulsed radio signal. Thus, for PSR B1828−11, the measured value of $\Delta I_d/I_C$ is

$$\frac{\Delta I_d}{I_C} = (\nu_s P_p)^{-1} = 9.2 \times 10^{-9} \left(\frac{511 \text{ days}}{P_p} \right) . \tag{14}$$

(We have included the factor 511 days$/P_p$ explicitly in case the precession period is actually ∼1009 or 256 days.)

3. ELASTIC DEFORMATION OF THE SLOWING CRUST: FORMALISM

Our goal in §§ 3 and 4 is to determine the rigidity parameter $b \equiv \Delta I_d/\Delta I_\Omega$ for a NS with a relaxed crust. We first show that ΔI_d can be reexpressed as the *difference* between (1) ΔI_Ω for a purely fluid NS and (2) ΔI_Ω for the same NS, but now having an elastic crust whose relaxed state is spherical. We then describe how we solve for ΔI_Ω for both cases 1 and 2, using perturbation theory.

Consider a two-parameter family of NSs, all with the same mass and composition and all spinning about the z-axis. The two parameters are the NS's actual angular velocity, Ω, and the angular velocity Ω_r at which its crust is relaxed. For convenience, we change the variables to Ω_r^2 and $\Delta\Omega^2 \equiv \Omega^2 - \Omega_r^2$. The star's inertia tensor $I_{\rm ab}$ is a function of both these variables: $I_{\rm ab} = I_{\rm ab}(\Omega_r^2,\ \Delta\Omega^2)$. By axial symmetry, we can write

$$I_{\rm ab} = I_0\left(\Omega_r^2,\ \Delta\Omega^2\right) g_{\rm ab} + I_2\left(\Omega_r^2,\ \Delta\Omega^2\right)\left(\hat{z}^a\hat{z}^b - \tfrac{1}{3} g_{\rm ab}\right) . \tag{15}$$

We define the function $\Delta I_d(\Omega)$ to be the "residual" I_2 of a NS that is nonrotating but whose crust is relaxed at angular velocity Ω. Then, by definition,

$$\Delta I_d(\Omega) \equiv I_2\left(\Omega^2,\ -\Omega^2\right) , \tag{16}$$

since $\Omega_r^2 = \Omega^2$ means that the crust is relaxed at angular velocity Ω and $\Delta\Omega^2 = -\Omega_r^2$ means that the star is nonrotating.

Note that $I_2(0,\ 0) = 0$, since $\Omega_r^2 = \Delta\Omega^2 = 0$ means both that the star's crust is relaxed and that the star is nonrotating, and hence the star is spherical. Therefore, we can write, to first order in Ω_r^2 and $\Delta\Omega^2$,

$$\Delta I_d(\Omega) \equiv I_2\left(\Omega^2,\ -\Omega^2\right) \tag{17}$$

$$= \Omega^2 \left.\frac{\partial I_2}{\partial(\Omega_r^2)}\right|_{0,0} - \Omega^2 \left.\frac{\partial I_2}{\partial(\Delta\Omega^2)}\right|_{0,0} \tag{18}$$

$$= I_2\left(\Omega^2,\ 0\right) - I_2\left(0,\ \Omega^2\right) . \tag{19}$$

This suggests our strategy for computing $\Delta I_d(\Omega)$: we compute both $I_2(\Omega^2, 0)$ and $I_2(0, \Omega^2)$ and take the difference. Now $I_2(\Omega^2, 0)$ is the I_2 of a star spinning at Ω, whose crust is completely relaxed at that spin. But if the crust is relaxed (i.e., if all shear stresses vanish), the shape of the star is the same as for a completely fluid star with the same mass and angular velocity. On the other hand, $I_2(0, \Omega^2)$ is the I_2 of a star whose angular velocity is Ω but whose crust is relaxed when spherical (i.e., when it is nonspinning).

Our computational strategy is to start with two nonspinning NSs, cases 1 and 2, identical except that case 1 is treated as a fluid throughout, while case 2 has an elastic crust whose relaxed shape is spherical. Now spin them both up to angular velocity Ω, calculate I_2 for each, and take the difference. The result is ΔI_d for a NS whose crust is relaxed at spin Ω. [More precisely, we find $\Delta I_d(\Omega)$, up to fractional corrections of the order of $\Omega^2 R^3/GM$.]

3.1. *The Perturbation Equations*

The advantage to the strategy outlined above is that *both* case 1 and case 2 can be treated with a linear analysis about a spherical background for the stellar structure, with centrifugal force acting as a source term that drives the star away from sphericity. The effect of centrifugal force is described by the following potential in spherical coordinates (with $\theta = 0$ corresponding to the rotation axis):

$$\delta\phi^c = -\tfrac{1}{2}\Omega^2 r^2\left(1 - \cos^2\theta\right) . \tag{20}$$

This potential has both an $l = 0$ and $l = 2$, $m = 0$ piece, $\delta\phi^c = \delta\phi_0^c + \delta\phi_2^c$, where

$$\delta\phi_0^c = -\tfrac{1}{3}\Omega^2 r^2 \tag{21}$$

and

$$\delta\phi_2^c(r,\ \theta,\ \phi) = \hat{\lambda} Y_{20}(\theta,\ \phi)\Omega^2 r^2 , \tag{22}$$

with

$$\hat{\lambda} \equiv \frac{1}{3}\sqrt{\frac{4\pi}{5}} . \tag{23}$$

The $l = 0$ piece causes spherically symmetric expansion of the star, while the $l = 2$ piece generates the equatorial bulge. Only the $l = 2$ piece contributes to I_2. However, displacements due to both the $l = 0$ and $l = 2$ pieces generate strains in the crust and, hence, are important in determining the maximum change in I_2 sustainable by the crust without cracking or otherwise relaxing. Previous work on spin-down–induced crustal strain (e.g., Baym & Pines 1971; Franco, Link, & Epstein 2000) considered incompressible NS models, where this issue does not arise since the $l = 0$ piece of the displacement vanishes for incompressible models. We now derive the equations governing the response of the star to any $\delta\phi^c$ and then specialize to the

$l = 2$ and $l = 0$ pieces separately. Note that our treatment is purely Newtonian.

3.1.1. *NS Response to Centrifugal Potential $\delta\phi^c$*

Inside the crust, the perturbed stress tensor $\delta\tau_{ab}$ (the sum of pressure and shear stresses) can be written as

$$\delta\tau_{ab} = -\delta p g_{ab} + 2\mu\sigma_{ab} , \tag{24}$$

where δ represents an Eulerian perturbation, $p(r)$ is the pressure, $\mu(r)$ is the crust's shear modulus, and σ_{ab} is the crust's strain tensor, defined by

$$\sigma_{ab} = \tfrac{1}{2}\left(\nabla_a\xi_b + \nabla_b\xi_a - \tfrac{2}{3}g_{ab}\nabla^c\xi_c\right) . \tag{25}$$

Here ξ^a is the displacement of the crust away from its relaxed state and ∇_a is the flat derivative operator associated with g_{ab}. The perturbation $\delta\tau_{ab}$ is determined by the condition of hydroelastic balance,

$$\nabla^a\delta\tau_{ab} = \delta\rho g\hat{\boldsymbol{r}}_b + \rho\nabla_b\left(\delta\phi + \delta\phi_2^c\right) , \tag{26}$$

where ρ is the density, $g(r) = GM_r/r^2$ is the local acceleration due to gravity, and $\hat{\boldsymbol{r}}_b$ is the radial unit vector. The perturbation $\delta\phi$ of the gravitational potential obeys

$$\nabla^2\delta\phi = 4\pi G\delta\rho . \tag{27}$$

Finally, the density change arising from the displacement ξ^a obeys the continuity equation,

$$\delta\rho = -\nabla^a(\rho\xi_a) . \tag{28}$$

The following boundary conditions arise from equation (26): (1) $\delta\tau_{r\perp}$ (where "$\perp$" refers to components orthogonal to the radial vector $\hat{\boldsymbol{r}}^a$) must go to zero at both the crust-core boundary and the stellar surface (using the fact that shear stresses vanish just outside the crust), and (2) $\delta\tau_{rr} = 0$ for perturbations that *break spherical symmetry* (since δp must vanish both in the liquid core—or else fluid would flow—and above the star). These conditions can be succinctly expressed as

$$\delta\tau_{ab}\hat{\boldsymbol{r}}^b = 0 \tag{29}$$

at both boundaries. (See Ushomirsky, Cutler, & Bildsten 2000, hereafter UCB, for a more detailed discussion of these boundary conditions.)

In the fluid core there are only two first-order equations to solve, for $\delta\phi$ and $d\,\delta\phi/dr$. To derive them, first note that equilibrium between pressure, gravitational, and centrifugal forces requires

$$\nabla_a\delta p = -\delta\rho\nabla_a\phi - \rho\nabla_a(\delta\phi + \delta\phi^c) . \tag{30}$$

Projecting equation (30) along the horizontal and radial directions, we have

$$\delta p(r) = -\rho(\delta\phi + \delta\phi^c) , \tag{31}$$

$$\frac{d\,\delta p}{dr} = -\delta\rho g - \rho\frac{d}{dr}(\delta\phi + \delta\phi^c) . \tag{32}$$

Taking d/dr of equation (31) and subtracting equation (32), we have

$$\delta\rho = g^{-1}\frac{d\rho}{dr}(\delta\phi + \delta\phi^c) , \tag{33}$$

so Poisson's equation becomes

$$\nabla^2\delta\phi = 4\pi G\left(g^{-1}\frac{d\rho}{dr}\right)(\delta\phi + \delta\phi^c) . \tag{34}$$

3.1.2. *$l = 2$ Deformations*

We now separate the above equations into spherical harmonics, thereby obtaining a system of first-order ordinary differential equations. Our treatment follows McDermott et al. (1988; see also UCB). Throughout this subsection, it is implicit that all scalar perturbations have Y_{20} angular dependence; we generally suppress explicit (l, m) subscripts on perturbed quantities.

We begin by writing the displacement vector ξ^a as the sum of radial and tangential pieces:

$$\xi^a \equiv \xi^r(r)\,Y_{lm}\hat{\boldsymbol{r}}^a + \xi^\perp(r)\beta^{-1}r\nabla^a Y_{lm}, \tag{35}$$

where $\hat{\boldsymbol{r}}^a$ is the unit radial vector and $\beta \equiv [l(l+1)]^{1/2}$. Then inside the crust, there are six variables:

$$\begin{aligned} z_1 &\equiv \frac{\xi^r}{r} , \quad z_2 \equiv \frac{\Delta\tau_{rr}}{p} = \frac{\delta\tau_{rr}}{p} - z_1\frac{d\ln p}{d\ln r} , \\ z_3 &\equiv \frac{\xi^\perp}{\beta r} , \quad z_4 \equiv \frac{\Delta\tau_{r\perp}}{\beta p} = \frac{\delta\tau_{r\perp}}{\beta p} , \\ z_5 &\equiv \frac{\delta\phi}{c^2}\frac{R^2}{r^2} , \quad z_6 \equiv \frac{dz_5}{d\ln r} , \end{aligned} \tag{36}$$

where δ and Δ refer to Eulerian and Lagrangian variations, respectively. The definitions of z_1–z_4 and $\delta\tau_{ab}$ are the same as in UCB. The above definition of z_5, with r^2 in the denominator, factors out the dominant behavior of $\delta\phi/c^2$ near $r = 0$.

The perturbation equations are (see McDermott et al. 1988; UCB)

$$\frac{dz_1}{d\ln r} = -\left(1 + 2\frac{\alpha_2}{\alpha_3}\right)z_1 + \frac{1}{\alpha_3}z_2 + 6\frac{\alpha_2}{\alpha_3}z_3 , \tag{37a}$$

$$\begin{aligned} \frac{dz_2}{d\ln r} = &\left(\tilde{U}\tilde{V} - 4\tilde{V} + 12\Gamma\frac{\alpha_1}{\alpha_3}\right)z_1 + \left(\tilde{V} - 4\frac{\alpha_1}{\alpha_3}\right)z_2 \\ &+ 6\left(\tilde{V} - 6\Gamma\frac{\alpha_1}{\alpha_3}\right)z_3 + 6z_4 \\ &+ \frac{\tilde{V}c_3}{Z_\star}(2z_5 + z_6) + 2\frac{\tilde{V}c_3}{Z_*}\hat{\lambda}\frac{R^2\Omega^2}{c^2} , \end{aligned} \tag{37b}$$

$$\frac{dz_3}{d\ln r} = -z_1 + \frac{1}{\alpha_1}z_4 , \tag{37c}$$

$$\begin{aligned} \frac{dz_4}{d\ln r} = &\left(\tilde{V} - 6\Gamma\frac{\alpha_1}{\alpha_3}\right)z_1 - \frac{\alpha_2}{\alpha_3}z_2 + \frac{2}{\alpha_3}\left(11\alpha_1\alpha_2 + 10\alpha_1^2\right)z_3 \\ &+ \left(\tilde{V} - 3\right)z_4 + \frac{\tilde{V}c_3}{Z_*}z_5 + \frac{\tilde{V}c_3}{Z_\star}\hat{\lambda}\frac{R^2\Omega^2}{c^2} , \end{aligned} \tag{37d}$$

$$\frac{dz_5}{d\ln r} = z_6 , \tag{37e}$$

$$\frac{dz_6}{d\ln r} = -5z_6 + \frac{\tilde{U}Z_*}{c_3}\left[\left(\frac{\tilde{V}}{\gamma} - 4\frac{\alpha_1}{\alpha_3}\right)z_1 - \frac{1}{\alpha_3}z_2 + 12\frac{\alpha_1}{\alpha_3}z_3\right] , \tag{37f}$$

where

$$\tilde{U} \equiv \frac{d\ln g}{d\ln r} + 2\ , \quad \tilde{V} \equiv \frac{\rho g r}{p} = -\frac{d\ln p}{d\ln r}\ , \quad \alpha_1 \equiv \frac{\mu}{p}\ ,$$
$$\Gamma = \left.\frac{\partial \ln p}{\partial \ln \rho}\right|_{\mu_e}\ , \quad \alpha_2 \equiv \Gamma - \frac{2}{3}\frac{\mu}{p}\ , \quad \alpha_3 \equiv \Gamma + \frac{4}{3}\frac{\mu}{p}\ ,$$
$$\gamma = \left.\frac{d\ln p}{d\ln \rho}\right|_{*}\ , \quad c_3 = \left(\frac{r}{R}\right)^3\left(\frac{M}{M_r}\right)\ , \quad Z_* = \frac{GM}{Rc^2}\ . \tag{38}$$

In the fluid, we rewrite equation (34) in terms of our dimensionless variables z_5 and z_6:

$$\frac{dz_5}{d\ln r} = z_6\ , \tag{39}$$
$$\frac{dz_6}{d\ln r} = -5z_5 - \frac{\tilde{U}\tilde{V}}{\gamma}\left(z_5 + \hat{\lambda}\frac{R^2\Omega^2}{c^2}\right)\ . \tag{40}$$

The boundary conditions are as follows. At the center of the star, $d\delta\phi/dr$ must vanish, giving

$$z_6 = 0\ , \tag{41}$$

while z_5 takes on an (unknown) finite value. At both the crust-core boundary ($r = r_c$) and the top of the crust ($r = R$), we have, from equation (29),

$$z_2 = \tilde{V}\left[\frac{\rho_l}{\rho_s}z_1 - \frac{c_3}{Z_*}\left(z_5 + \hat{\lambda}\frac{R^2\Omega^2}{c^2}\right)\right]\ ,$$
$$z_4 = 0\ . \tag{42}$$

In addition, at the top of the crust ($r = R$),

$$5z_5 + z_6 = 0\ . \tag{43}$$

Finally, at the crust-core boundary $\delta\phi$ and $d\delta\phi/dr$ must be continuous, requiring that z_5 and z_6 are as well. We thus have eight equations (two in the core and six in the crust) and eight boundary conditions (one at the center, three at the surface, and four at the crust-core boundary). For simplicity, we set the outer boundary of the NS at the top of the crust. For convenience, we approximate Γ as γ in equation (37) (i.e., we do not distinguish $d\ln p/d\ln\rho$ of the background model from the derivative at constant composition). Solutions of these equations are described in § 4.

The I_2 of the NS's inertia tensor is related to the NS's quadrupole moment Q_{20} by

$$I_2 = \sqrt{\frac{4\pi}{5}}Q_{20}\ , \tag{44}$$

where Q_{20} is defined as

$$Q_{20} \equiv \int \delta\rho(r) r^4\, dr\ . \tag{45}$$

Q_{20} is related to z_5 at the NS surface by

$$Q_{20} = -\frac{5c^2}{4\pi G}z_5|_{r=R}\ . \tag{46}$$

As a check on the accuracy of our solutions, we also calculate Q_{20} directly from the following integrals. In the crust, $\delta\rho = -\boldsymbol{\nabla}\cdot(\rho\boldsymbol{\xi})$, so

$$Q_{20}^{\rm crust} = 2\int_{r_c}^{R}\rho(z_1 + 3z_3)r^4 dr - \left[r^5\rho z_1\right]_{r=r_c}^{r=R} \tag{47}$$
$$= \frac{MR^2}{4\pi}\left\{2\int_{r_c}^{R}\frac{\tilde{U}}{c_3}(z_1+3z_3)\left(\frac{r}{R}\right)^5 d\ln r - \left[\left(\frac{r}{R}\right)^5\frac{\tilde{U}}{c_3}z_1\right]_{r=r_c}^{r=R}\right\}\ . \tag{48}$$

In the liquid part of the star, we use equation (33) to obtain

$$Q_{20}^{\rm fluid} = -\frac{MR^2}{4\pi Z_\star}\int_0^{r_c}\frac{\tilde{U}\tilde{V}}{\gamma}\left(z_5 + \hat{\lambda}\frac{R^2\Omega^2}{c^2}\right)\left(\frac{r}{R}\right)^5 d\ln r\ . \tag{49}$$

In a star with both crust and core, we take $Q_{20} = Q_{20}^{\rm fluid} + Q_{20}^{\rm crust}$. In practice, we refine our numerical solution until the sum of equations (48) and (49) agrees with equation (46) to within required tolerance—about one part in 10^{10}.

To find Q_{20} for a purely fluid star, we solve the same fluid equations, but instead of matching at the bottom of the crust, we impose the boundary condition equation (43) at $r = R$. Neither solution 1 nor 2 is really accurate to one part in 10^{10} because we approximate the star's outer boundary as being at the top of the crust (ignoring the thin ocean on top) and because we approximate Γ by γ in equation (37). However, since we use the same approximations in the solutions to both problems 1 and 2, the *difference* is due solely to the presence of an elastic crust in model 2. Therefore, we claim we do know difference between cases 1 and 2 to three significant figures despite the fact that the two quantities agree to seven significant figures. This claim is checked in Appendix A, where we obtain an approximate analytical expression for b.

3.1.3. $l = 0$ *Deformations*

The $l = 0$ component of the centrifugal potential, $\delta\phi_0^c$, generates a spherically symmetric radial displacement field $\xi^a = \xi^r(r)\hat{r}^a$, as well as pressure, density, and gravitational potential perturbations. In this subsection, all scalar perturbed quantities are purely functions of r.

In order to compute ξ^r for the $l = 0$ case, we neglect the small shear modulus of the crust (effectively taking the entire star to be fluid). Of course, it is the small shear modulus that determines ΔI_d, and so in the previous subsection our equations included it. However, our present purpose is only to determine (roughly) the $l = 0$ piece of the crustal strain resulting from NS spin-down, and for this we can neglect μ, since it has only a small influence on the radial displacement. This approximation is justified by the smallness of the crust's shear modulus compared to the pressure. With this approximation, the perturbations in pressure, density, and gravitational potential obey

$$\frac{d\,\delta p}{dr} = -\delta\rho\ g - \rho\frac{d}{dr}(\delta\phi + \delta\phi_0^c)\ , \tag{50}$$
$$\frac{\delta p}{p} = \Gamma\frac{\delta\rho}{\rho} + (\gamma - \Gamma)\xi^r\frac{d\ln\rho}{dr}\ , \tag{51}$$
$$\nabla^2\delta\phi = 4\pi G\delta\rho\ . \tag{52}$$

Equation (51) comes from setting $(\Delta p/p) = \Gamma(\Delta\rho/\rho)$.

We define dimensionless variables

$$y_1 \equiv \frac{\xi^r}{r} , \quad y_2 \equiv \frac{\delta p}{p} ,$$
$$y_3 \equiv \frac{\delta\phi}{c^2} , \quad y_4 \equiv \frac{dy_3}{d\ln r} , \tag{53}$$

and obtain

$$\frac{dy_1}{d\ln r} = \left(\frac{\tilde{V}}{\gamma} - 3\right) y_1 - \frac{1}{\gamma} y_2 , \tag{54a}$$

$$\frac{dy_2}{d\ln r} = \tilde{V}\left(1 - \frac{1}{\gamma}\right) y_2 - \frac{\tilde{V} c_3}{Z_\star}\left[y_4 \left(\frac{R}{r}\right)^2 - \frac{2}{3}\frac{R^2\Omega^2}{c^2}\right] , \tag{54b}$$

$$\frac{dy_3}{d\ln r} \equiv y_4 , \tag{54c}$$

$$\frac{dy_4}{d\ln r} \equiv \frac{\tilde{U} Z_*}{c_3 \gamma}\left(\frac{r}{R}\right)^2 y_2 - y_4 . \tag{54d}$$

Boundary conditions at $r = 0$ are obtained from the requirement that the solution be regular there. This yields

$$\left(4 - \frac{\Gamma}{\gamma}\right) y_1 + \frac{1}{\Gamma} y_2 = 0 \quad \text{and} \quad y_4 = 0 . \tag{55}$$

At $r = R$, Δp must vanish and the gravitational potential must match onto its solution in empty space ($\delta\phi \propto 1/r$), so there

$$y_2 - \tilde{V} y_1 = 0 \quad \text{and} \quad y_3 + y_4 = 0, \tag{56}$$

while y_3 and y_4 are continuous at the crust-core interface.

4. ELASTIC DEFORMATION OF THE SLOWING CRUST: RESULTS

In this section, we describe the solutions to the elastic perturbation equations derived in § 3, present our results for the value of $b = \Delta I_d / I_\Omega$, and compare it to the Baym-Pines estimate, equation (3).

In order to solve the perturbation equations, we need to specify the background NS model. We build NS models using several representative equations of state (EOSs), summarized in Table 1. These models vary somewhat in their treatment of the pressure-density relation in the core and the crust. In particular, model FPS uses the EOS described in Lorenz, Ravenhall, & Pethick (1993); model WS uses EOS UV14+TNI of Wiringa, Fiks, & Fabrocini (1988) in the core, matched to model FPS in the crust. Models AU and UU use EOSs AV14+UVII and UV14+UVII, respectively, matched to the EOS of Negele & Vautherin (1973) in the crust. In practice, we use tabulations of pressure versus density provided with the code RNS.[1] Finally, model n1poly uses a pressure-density relation of an $n = 1$ polytrope throughout the star. In all cases, we assume zero temperature, take $M = 1.4\ M_\odot$, and construct the NS model by solving the purely Newtonian equations of hydrostatic balance, $dp/dr = -\rho g$, and continuity, $dM_r/dr = 4\pi r^2 \rho$. The resulting NS parameters (radius, I_0, I_C, and $\Delta I_\Omega/\Omega^2$) are shown in Table 1.

In this paper we generally assume that I_C equals the moment of inertia of the crustal nuclei (i.e., excluding the dripped neutrons in the inner crust), which is roughly 1% of I_0, since estimates of frictional coupling give coupling times between the crust and core well in excess of the spin period (see, e.g., Alpar & Sauls 1988). If the stellar magnetic field penetrates the core, magnetic stresses will also play a role in the coupling (Abney, Epstein, & Olinto 1996; Mendell 1998), but the magnetic coupling timescale (estimated as the Alfvén crossing time for waves in the core) is again much longer than the rotation period for most NSs. However, it is possible that some process *does* strongly couple the core to crust (in which case I_C could be a substantial fraction of I_0), so we shall indicate how our main results scale with I_C/I_0.

In all models, we place the crust-core boundary at the fiducial density of $\rho_b = 1.5 \times 10^{14}$ g cm^{-3} (Lorenz et al. 1993). The crust-ocean boundary is placed at $\rho = 10^9$ g cm^{-3} for all models except for the $n = 1$ polytrope one, where it is placed at 10^{11} g cm^{-3} in order to ensure numerical stability of our integration of the elastic equations.[2]

We use the shear modulus μ as computed by Strohmayer et al. (1991), via Monte Carlo simulations of both bcc crystals and quenched solids. Their results can be conveniently rewritten in terms of the pressure p_e of degenerate relativistic electrons,

$$\frac{\mu}{p_e} = \frac{6 \times 10^{-3}}{1 + 0.595(173/\Gamma_{\rm Coul})^2}\left(\frac{Z}{8}\right)^{2/3} , \tag{57}$$

where $\Gamma_{\rm Coul} = Z^2 e^2/akT$ is the ratio of the Coulomb energy of the lattice to the thermal energy and Z is the ionic charge. Throughout most of the crust (i.e., except near the top) $\Gamma_{\rm Coul} > 10^3$, so for simplicity we ignore the slight

[1] See N. Stergioulas, at http://www.gravity.phys.uwm.edu/rns.

[2] In the $n = 1$ polytrope model, the density falls of very rapidly with radius in the outer layers—much faster than in models with a more realistic EOS. This very rapid variation over many orders of magnitude causes numerical problems. However, this truncation does not affect the final results since the outer crust contains a negligible fraction of the mass.

TABLE 1
SUMMARY OF NS MODELS, COMPUTED b-VALUES, AND CRUSTAL STRAINS

EOS	R (km)	I_0 ($\times 10^{45}$ g cm^2)	I_C/I_0 ($\times 10^{-2}$)	$\Delta I_\Omega/I_0$ [$\times(\nu_s$/kHz)^2]	b Actual	b Baym-Pines	$\bar{\sigma}_{\rm pole}$	$\bar{\sigma}_{\rm ave}$
AU	12.13	1.11	0.86	0.259	2.47×10^{-7}	9.20×10^{-6}	17.1	0.457
UU	12.78	1.23	1.11	0.302	4.20×10^{-7}	1.25×10^{-5}	18.9	0.495
FPS	11.97	1.05	0.78	0.241	1.70×10^{-7}	8.09×10^{-6}	16.7	0.432
WS	12.05	1.10	0.70	0.257	1.47×10^{-7}	7.62×10^{-6}	14.9	0.449
n1poly	12.53	1.15	2.86	0.275	1.31×10^{-5}	2.14×10^{-4}	103	0.502

NOTE.—Summarizes our results on the crustal rigidity and spin-down strain for five different EOSs and compares to the Baym-Pines estimate for b. The average value of the spin-down strain $\bar{\sigma}^{\rm sd}_{\rm ave}$ and its maximum value $\bar{\sigma}^{\rm sd}_{\rm pole}$ (attained on the spin axis, near the north pole) are both normalized to $R\Omega/c = 1$. Results here assume the density at the bottom is $\rho_b = 1.5 \times 10^{14}$ g cm^{-3}.

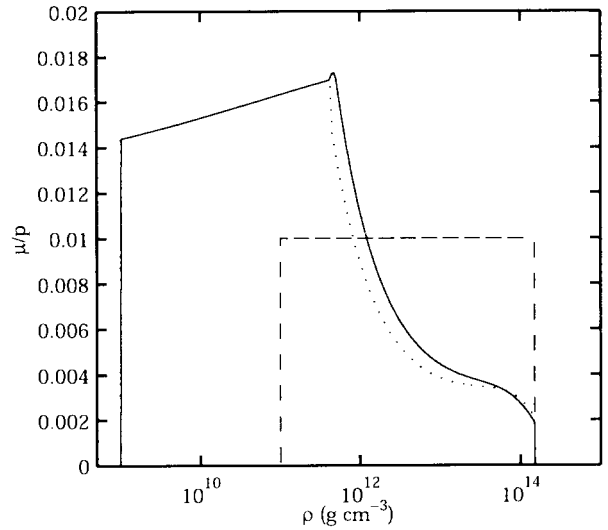

FIG. 2.—Ratio of the shear modulus to the pressure as a function of density for the NS models used in this paper: models AU (*solid line*), WS (*dotted line*), n1poly (*dashed line*).

dependence of the shear modulus on temperature, effectively setting $1/\Gamma_{\rm Coul}$ equal to 0. In order to compute the composition (A and Z of nuclei, as well as the free neutron fraction) we use the fits of Kaminker et al. (1999) to the formalism of Oyamatsu (1993). The resulting run of μ with density is shown in Figure 2. For the $n = 1$ polytrope model, we use a fiducial value of $\mu/p = 10^{-2}$.

With the background model specified as above, we solve the perturbation equations of § 3 using relaxation with adaptive mesh allocation (see, e.g., Press et al. 1992 for a description). For the case of $l = 2$ perturbations in a purely fluid star, as well as for $l = 0$ perturbations, the solution is straightforward. However, for $l = 2$ perturbations in a star with a crust, there are internal boundary conditions at the crust-core interface (eq. [42]), which makes application of the standard relaxation method more complicated. In this case, to deal with this internal boundary, we transform the independent variable from $x = \ln r$ to t, such that for the fluid part of the star $x = (x_c - x_0)t + x_0$, while in the crust $x = x_1 - (x_1 - x_c)t$, where x_0, x_1, and x_c are the values near the center, at the crust-ocean boundary, and at the crust-core boundary, respectively. With this change of the independent variable, *both* the fluid and crust equations can be solved simultaneously on the interval $t \in [0,\ 1]$: the internal boundary conditions are eliminated.

In Figure 3 we show the radial and transverse displacements induced when a relaxed, nonrotating star is spun up to $\Omega = c/R$. [This is the solution of our perturbation equations with $(R\Omega/c)^2$ set equal to 1 in our source term eq. (20)]. Of course, $\Omega = c/R$ is an unreasonably large spin value, but our solutions scale linearly with the source term, i.e., quadratically in Ω, so in all applications we simply scale the results down to low Ω. Recall that, when solving the elastic perturbation equations, we imagine taking a spherically symmetric star and spinning it up. In this case, the $l = 0$ part of the centrifugal force acts radially outward, and hence the $l = 0$ component of the radial displacement (bottom panel of Fig. 3) is positive throughout the crust. On the other hand, the $l = 2$ part of the centrifugal force squeezes the crust at the poles and pushes it out at the equator. Hence, z_1

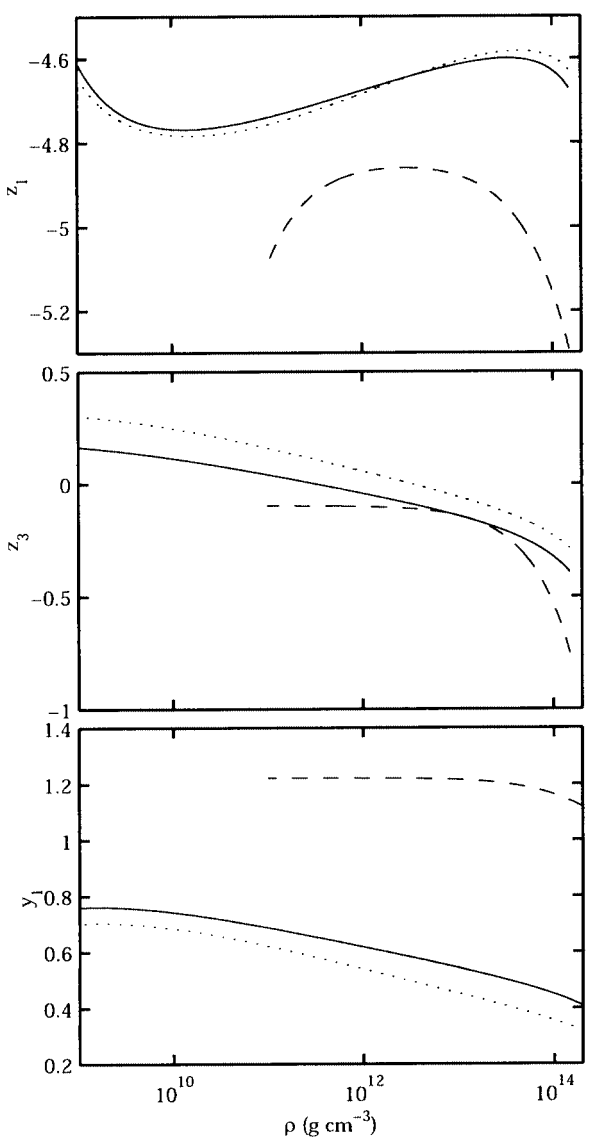

FIG. 3.—Crustal displacements for a relaxed, nonrotating NS that is spun up to $\Omega = c/R$. The different curves represent different EOSs: models AU (*solid lines*), WS (*dotted lines*), and n1poly (*dashed lines*). For $\nu_{s,\rm ref} = 40$ Hz, the values in this plot must be multiplied by 6.5×10^{-5}. *Top*: $l = 2$ radial displacement z_1. *Middle*: $l = 2$ transverse displacement z_3. *Bottom*: $l = 0$ radial displacement y_1.

(top panel of Fig. 3), which can be thought of as the radial displacement at the poles [times $R^{-1}(4\pi/5)^{1/2}$], is negative. The transverse displacement, z_3 (middle panel of Fig. 3), changes sign in order to satisfy mass continuity.

Adding the $l = 0$ and $l = 2$ perturbations, we can rewrite the strain tensor (eq. [25]) as

$$\sigma_{\rm ab} = (\sigma_0 + \sigma_{rr} Y_{20})(\hat{r}_a \hat{r}_b - \tfrac{1}{2} e_{\rm ab}) + \sigma_{r\perp} f_{\rm ab} + \sigma_\Lambda (\Lambda_{\rm ab} + \tfrac{1}{2} e_{\rm ab}) \ . \tag{58}$$

Here the tensors $e_{\rm ab}$, $f_{\rm ab}$, and $\Lambda_{\rm ab}$ are defined by

$$e_{\rm ab} \equiv g_{\rm ab} - \hat{r}_a \hat{r}_b \ , \tag{59a}$$

$$f_{\rm ab} \equiv \beta^{-1} r (\hat{r}_a \nabla_b Y_{lm} + \hat{r}_b \nabla_a Y_{lm}) \ , \tag{59b}$$

$$\Lambda_{\rm ab} \equiv \frac{r^2}{l(l+1)} \nabla_a \nabla_b Y_{lm} + f_{\rm ab} \ , \tag{59c}$$

the $l = 2$ strain components σ_{rr}, $\sigma_{r\perp}$, and σ_Λ are given by

$$\sigma_{rr}(r) = \frac{2}{3}\frac{dz_1}{d\ln r} + \frac{1}{3}\beta^2 z_3 \ , \tag{60a}$$

$$\sigma_{r\perp}(r) = \frac{\beta^2 z_4}{2\mu} \ , \tag{60b}$$

$$\sigma_\Lambda(r) = \beta^2 z_3 \ , \tag{60c}$$

and the $l = 0$ piece is

$$\sigma_0 = \frac{2}{3}\frac{dy_1}{d\ln r} \ . \tag{61}$$

In Figure 4 we show the radial functions σ_{rr} (*top panel*), $\sigma_{r\perp}$ (*second panel*), σ_Λ (*third panel*), and σ_0 (*bottom panel*), for EOSs AU, WS, and n1poly. Again, these results are normalized to $(R\Omega/c)^2 = 1$.

The crust breaks (or deforms plastically) when

$$\bar{\sigma} \equiv \left(\tfrac{1}{2}\sigma_{\rm ab}\sigma^{\rm ab}\right)^{1/2} > \bar{\sigma}_{\rm max} \ , \tag{62}$$

where $\bar{\sigma}_{\rm max}$ is the *yield strain*. (This is the von Mises criterion; see § 6 of UCB for a discussion.) From equation (58), we get

$$2\bar{\sigma}^2 = \frac{3}{2}(\sigma_0 + \sigma_{rr}Y_{20})^2 + \sigma_{r\perp}^2\frac{5}{64\pi}(\sin 2\theta)^2 + \sigma_\Lambda\frac{5}{32\pi}\sin^4\theta \ , \tag{63}$$

where $Y_{20} = (5/16\pi)^{1/2}(3\cos^2\theta - 1)$; $\bar{\sigma}$ is independent of ϕ by symmetry. In Figure 5 we plot contours of $\bar{\sigma}$ on a meridional plane (i.e., a plane that slices through the crust of the star at a constant longitude ϕ), and in Figure 6 we show $\bar{\tau} = 2\mu\bar{\sigma}$, again on a meridional plane. Clearly, the stresses are largest at the base of the crust, where μ is largest, while the strains are highest at the top of the crust (where they cost the least, energetically).

In Table 1 we show the value of b computed as described in § 3 using the solutions to the perturbation problem and compare them to the estimates of Baym & Pines (1971) given by equation (3). Equation (3) overestimates b by a factor of 15–50. To emphasize this difference, and also to explore its dependence on ρ_b (the assumed density at the crust-core boundary), we show in Figure 7 the ratio of our calculated b to the Baym-Pines estimate as a function of ρ_b. In the two appendices, we explore why the estimate, equation (3), is inaccurate. Briefly, when a uniform elastic sphere spins down, its strain energy is strongly concentrated toward the center of the star; thus, this case (on which eq. [3] is based) is unsuitable for estimating the rigidity of a realistic NS, where all the strain energy is near the surface, in the thin crust. Moreover, we show that in a realistic NS crust,

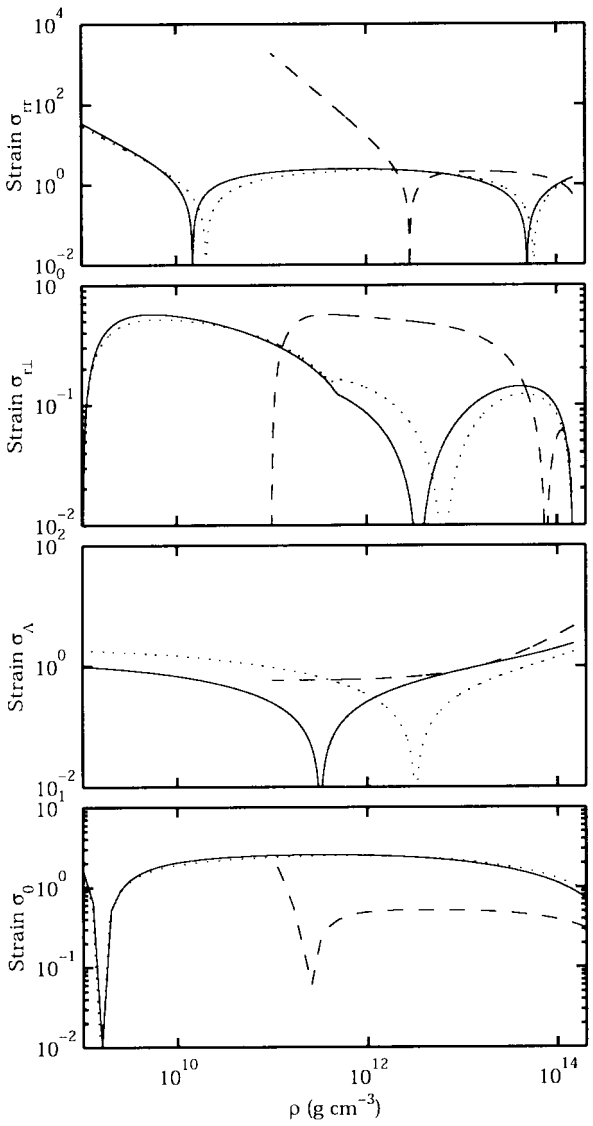

FIG. 4.—Radial dependence of the (spin-down portion of the) strain tensor for models AU (*solid line*), WS (*dotted line*), and n1poly (*dashed line*), normalized to $\Omega = c/R$. For $\nu_{s,\rm ref} = 40$ Hz, the values in this plot must be multiplied by 6.5×10^{-5}. *Top panel*: $|\sigma_{rr}|$. *Second panel*: $|\sigma_{r\perp}|$. *Third panel*: $|\sigma_\Lambda|$. *Bottom panel*: $|\sigma_0|$. The signs of the components are as follows. At the bottom of the crust, for all three EOSs: $\sigma_{r\perp} > 0$, $\sigma_\Lambda < 0$, and $\sigma_0 > 0$; $\sigma_{rr} > 0$ at the bottom for the AU and WS models, but $\sigma_{rr} < 0$ there for the n1poly model. The sharp dips in the figures are zero crossings.

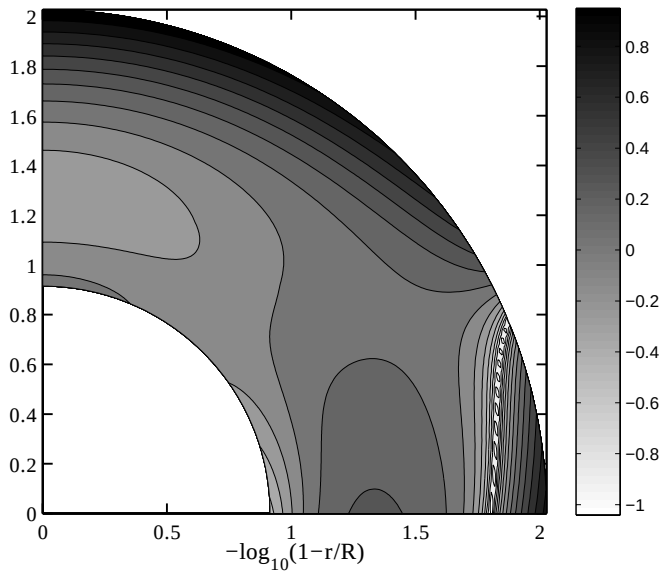

FIG. 5.—Distribution of (spin-down portion of the) crustal strain $\bar{\sigma}$ on a slice in a meridional plane, containing the rotation axis (pointing upward) for model AU. Results are normalized to $\Omega = c/R$. Gray scale indicates $\log_{10}\bar{\sigma}$.

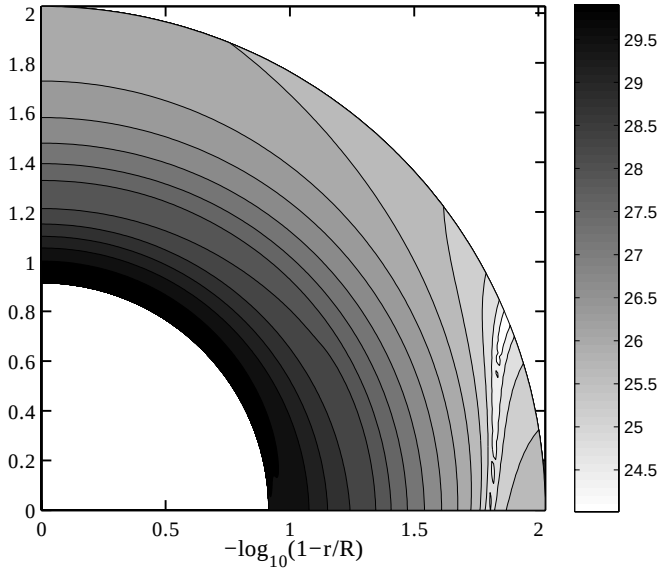

FIG. 6.—Distribution of (the spin-down portion of the) crustal shear stress $\bar{\tau}$ on a slice in a meridional plane, containing the rotation axis (pointing upward) for model AU. Results are normalized to $\Omega = c/R$. Gray scale indicates $\log_{10} \bar{\tau}$, where $\bar{\tau}$ is in cgs units (ergs cm^{-3}).

contributions to ΔI_d from different stress components and different depths cancel each other to a much higher degree than one might expect from consideration of a uniform, incompressible crust.

5. ΔI_d FOR NONRELAXED CRUSTS

So far in this paper we have calculated the residual oblateness ΔI_d that a spinning NS with a *relaxed* crust retains if it is gently torqued down to zero spin frequency. But a real NS that is spinning down (or spinning up, because of accretion) is probably not completely relaxed. Indeed, we see below that the precession frequency of PSR B1828−11 is inconsistent with the assumption of a relaxed crust (assuming that shear stresses are indeed responsible for this NS's ΔI_d). The crust, because it has finite rigidity, becomes strained as its spin changes. (As shown in Fig. 4 and § 6, if no cracking or relaxation occurs, then the strain near the top of the crust grows to rather large values; e.g., for PSR B1828−11, the strain near the top would be $\sim 10^{-3}$ in this case.) In some portions of the crust, the strain could be relaxed in localized episodes of crust cracking (star quakes) or plastic flow, while in other regions the strain may simply build up. Precisely because the NS crust may have a complex history of strain buildup and release, its current strain pattern is impossible to predict exactly.

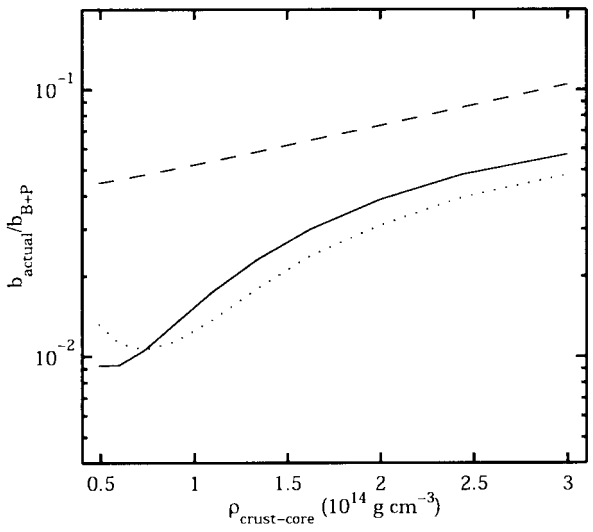

FIG. 7.—Ratio of energy in crustal stresses to that in centrifugal stresses, b, scaled to the Baym-Pines estimate, plotted as a function of the location of the crust-core boundary for models AU (*solid line*), WS (*dotted line*), and n1poly (*dashed line*).

Fortunately, however, many of our results can immediately be generalized to this case of a nonrelaxed crust, by scaling them to the crust's "reference spin" $\nu_{s,\mathrm{ref}}$, defined as follows. We imagine adjusting the NS's spin frequency ν_s while keeping the crust's preferred (zero-strain) shape fixed (i.e., without letting the crust crack or otherwise relax). While in general there will be no spin at which the crust is completely relaxed, if we plot the resulting quadrupole moment Q_{20} as a function of ν_s, there would be one spin value, $\nu_{s,\mathrm{ref}}$, such that $Q_{20}(\nu_{s,\mathrm{ref}})$ was identical to the Q_{20} of a perfect-fluid NS with the same mass and spin, $\nu_{s,\mathrm{ref}}$. (Here we are making the natural assumption that the crust's preferred shape is roughly oblate, as opposed to prolate.) We define the crustal strain field at $\nu_{s,\mathrm{ref}}$ to be $\sigma_{\mathrm{ab}}^{\mathrm{ref}}$. While $\sigma_{\mathrm{ab}}^{\mathrm{ref}}$ is in general nonzero, these strains make no net contribution to the NS's quadrupole moment. In a rough way, one can think of $\nu_{s,\mathrm{ref}}$ as the spin at which the crust is *most relaxed.* As an example, consider a NS that is born with a relaxed crust at spin $\nu_{s,\mathrm{init}}$ and never relaxes at all as it spins down to $\nu_{s,\mathrm{final}}$. Then $\nu_{s,\mathrm{ref}} = \nu_{s,\mathrm{init}}$ and $\sigma_{\mathrm{ab}}^{\mathrm{ref}} = 0$. If, on the other hand, the NS relaxes somewhat (but not completely) as it spins down, then $\nu_{s,\mathrm{ref}}$ will lie somewhere between $\nu_{s,\mathrm{init}}$ and $\nu_{s,\mathrm{final}}$, and one would generally expect $\sigma_{\mathrm{ab}}^{\mathrm{ref}} \neq 0$.

The point of these definitions is the following. Imagine a NS with strained crust and spin ν_s. To determine this NS's precession frequency, we want to know what residual oblateness ΔI_d it would have if it were spun down to zero frequency. We can imagine accomplishing the spin-down in two steps. First, adjust the spin to $\nu_{s,\mathrm{ref}}$. At this spin, the crust has some strain $\sigma_{\mathrm{ab}}^{\mathrm{ref}}$, but $\sigma_{\mathrm{ab}}^{\mathrm{ref}}$ has no net effect on the NS's oblateness. Second, we spin the star down from $\nu_{s,\mathrm{ref}}$ to zero angular velocity. We define $\sigma_{\mathrm{ab}}^{\mathrm{sd}}$ to be the extra strain that this spin-down induces; i.e., $\sigma_{\mathrm{ab}}^{\mathrm{sd}} \equiv \sigma_{\mathrm{ab}} - \sigma_{\mathrm{ab}}^{\mathrm{ref}}$, where σ_{ab} is the strain in the NS when it is nonrotating. Conceptually, we can consider both $\sigma_{\mathrm{ab}}^{\mathrm{ref}}$ and $\sigma_{\mathrm{ab}}^{\mathrm{sd}}$ as independent, small (i.e., linear) perturbations and work to first order in both. To this order, $\sigma_{\mathrm{ab}}^{\mathrm{sd}}$ is just the strain induced when spinning down a relaxed NS from $\nu_{s,\mathrm{ref}}$ to zero spin, which we solved for in § 4. Also to this order, the oblateness ΔI_d caused by σ_{ab} is the sum of (*a*) the oblateness due to $\sigma_{\mathrm{ab}}^{\mathrm{sd}}$ and (*b*) the oblateness due to $\sigma_{\mathrm{ab}}^{\mathrm{ref}}$, but term *b* vanishes, by definition. That is, ΔI_d is just the oblateness induced by the spin-down part of the strain field, Thus, generalizing equation (1), we can write

$$\Delta I_d = b \Delta I_\Omega\left(\nu_{s,\mathrm{ref}}\right) , \tag{64}$$

where $\Delta I_\Omega(\nu_{s,\mathrm{ref}}) \approx 0.3 I_0 \left(\nu_{s,\mathrm{ref}}/\mathrm{kHz}\right)^2$ is the oblateness of a fluid star with spin $\nu_{s,\mathrm{ref}}$ and b is the same coefficient (i.e., same numerical value) we calculated in § 3.

6. THE PRECESSION FREQUENCY OF PSR B1828−11

In § 2 we showed that the measured precession period of PSR B1828−11 implies that, for this NS,

$$\left.\frac{\Delta I_d}{I_C}\right|_{1828} = 9.2\times10^{-9}\left(\frac{511\text{ days}}{P_p}\right) . \tag{65}$$

For a NS with relaxed crust (i.e., relaxed except for the stresses induced by precessional motion itself), the predicted value is

$$\frac{\Delta I_d}{I_C} = b\frac{\Delta I_\Omega}{I_0}\left(\frac{I_C}{I_0}\right)^{-1} . \tag{66}$$

From the results of § 4, we estimate (for our Newtonian NS models)

$$\frac{\Delta I_\Omega}{I_0} \approx 0.3\left(\frac{\nu_s}{\text{kHz}}\right)^2\left(\frac{M}{1.4\ M_\odot}\right)^{-1}\left(\frac{R}{12\text{ km}}\right)^3 , \tag{67}$$

$$\frac{I_C}{I_0} \approx 0.01\left(\frac{M}{1.4\ M_\odot}\right)^{-2}\left(\frac{R}{12\text{ km}}\right)^4 , \tag{68}$$

$$b \approx 2\times10^{-7}\left(\frac{M}{1.4\ M_\odot}\right)^{-3}\left(\frac{R}{12\text{ km}}\right)^5 . \tag{69}$$

The scaling with NS mass and radius are estimated by taking (*a*) $\Delta I_\Omega/I_0 \propto MR^2/(M^2/R) = R^3/M$ (i.e., to the ratio of the NS's kinetic and potential energies), (*b*) $I_C/I_0 \propto M_C/M \propto \rho_{\rm bot}R^2\Delta R/M \propto R^2p_{\rm bot}/(gM) \propto R^4/M^2$, and (*c*) $b \propto \mu_{\rm ave}V_C/(M^2/R) \propto R^2\Delta R\,/(M^2/R) \propto R^2[p_{\rm bot}/(g\rho_{\rm bot})]/(M^2/R) \propto R^5/M^3$. Here M_C is the mass of the crust, ΔR is its thickness, V_C its volume, $\rho_{\rm bot}$ and $p_{\rm bot}$ are the density and pressure at the bottom of the crust, $\mu_{\rm ave}$ is a volume-weighted average of the crustal shear modulus, and $g \equiv GM/R^2$.

Taking $\nu_s = 2.5$ Hz, we estimate for PSR B1828−11

$$\left.\frac{\Delta I_d}{I_C}\right|_{\rm relaxed} \approx 3.8\times10^{-11}\frac{I_C/I_0}{10^{-2}}\left(\frac{M}{1.4\ M_\odot}\right)^{-2}\left(\frac{R}{12\text{ km}}\right)^4 . \tag{70}$$

Note that the measured value, equation (65), is ∼250 times larger than our relaxed-crust estimate for our fiducial NS parameters and precession period. And note that if some substantial fraction of the core is dynamically coupled to the crust (so $I_C \gg 0.01I_0$), then the discrepancy only gets worse. Even if we assume that PSR B1828−11's precession period is really ∼1000 days and take rather extreme values for the NS mass and radius, $M = 1.0\ M_\odot$ and $R = 20$ km, we are still left with a factor of ∼8 discrepancy. We conclude that either our basic picture is wrong (i.e., either PSR B1828−11 is not actually precessing or some other mechanism *besides* crustal shear stress is responsible for its large ΔI_d) or the crust is *not* relaxed. Here we adopt the latter explanation and pursue its implications.

The 511 day precession period for PSR B1828−11 implies that the star's reference spin is 40 Hz. Subsequent spin-down to its present spin of 2.5 Hz without significant structural relaxation (through quakes or plastic flow) would strain the crust and give the inferred $\Delta I_d/I_C = 9.2\times10^{-9}$. What are the current strain levels in the crust of PSR B1828−11 in this scenario? Compared to 40 Hz, its current spin of 2.5 Hz is very slow. If one continued slowing PSR B1828−11 down to zero angular velocity, the spin-down–induced crustal stresses would increase fractionally by only 0.4%. So (neglecting that 0.4%), the current strains are the sum of (*a*) the reference strain $\sigma_{\rm ab}^{\rm ref}$ that this NS would still have if it were spun up to $\nu_s = 40$ Hz and (*b*) the spin-down strains $\sigma_{\rm ab}^{\rm sd}$ induced by spinning a relaxed NS down from $\nu_s = 40$ to 0 Hz. While $\sigma_{\rm ab}^{\rm ref}$ is practically unknowable, the spin-down–induced strains $\sigma_{\rm ab}^{\rm sd}$ are those we found in § 4.

We parameterize the strength of the spin-down strain $\sigma_{\rm ab}^{\rm sd}$ by the scalar quantity $\bar\sigma^{\rm sd}$, defined by

$$\bar\sigma^{\rm sd} \equiv \left(\tfrac{1}{2}\sigma_{\rm ab}^{\rm sd}\sigma^{\rm sd,ab}\right)^{1/2} , \tag{71}$$

and we define the μ-weighted average of the crustal spin-down strain, $\bar\sigma_{\rm ave}$, by

$$\bar\sigma_{\rm ave}^{\rm sd} \equiv \frac{\int\mu\bar\sigma\,dV}{\int\mu\,dV} . \tag{72}$$

We have computed $\bar\sigma_{\rm ave}^{\rm sd}$ for our five EOSs; the results are in Table 1. They all give roughly the same result: $\bar\sigma_{\rm ave}^{\rm sd} \approx 0.5$ for $R\Omega/c = 1$. Scaling to the 40 Hz reference angular velocity of PSR B1828−11 yields

$$\bar\sigma_{\rm ave}^{\rm sd} = 5\times10^{-5}\left(\frac{P_s}{0.4\text{ s}}\right)\left(\frac{P_p}{511\text{ days}}\right)^{-1} \times\left(\frac{I_C/I_0}{0.01}\right)\left(\frac{b}{2\times10^{-7}}\right)^{-1} . \tag{73}$$

Again, the total strain $\sigma_{\rm ab}$ is the sum of $\sigma_{\rm ab}^{\rm sd}$ and $\sigma_{\rm ab}^{\rm ref}$, where $\sigma_{\rm ab}^{\rm ref}$ is determined by the detailed evolution of the crust, through structural adjustments, and so without knowing that history we can say nothing definitive about $\sigma_{\rm ab}^{\rm ref}$ (except that, by definition, these strains have no net effect on the NS's quadrupole moment). However, since $\sigma_{\rm ab}^{\rm ref}$ will contain contributions from all harmonics (i.e., all Y_{lm}), while $\sigma_{\rm ab}^{\rm sd}$ is wholly $l = 2, m = 0$, it seems quite likely that the NS's average total strain is larger than the average spin-down strain. *If* this is true, the average value of the spin-down portion of the strain places a lower limit on the crustal breaking strain: $\bar\sigma_{\rm max} \gtrsim 5\times10^{-5}(511\text{ days}/P_p)$. In terrestrial solids, strains of the order of 5×10^{-5} are rather easy to maintain, so it seems likely that the NS crust is strong enough to sustain the ΔI_d implied by the precession frequency.

If I_C/I_0 is of the order of unity, the implied average strain would be $\bar\sigma_{\rm ave} \gtrsim 5\times10^{-3}(511\text{ days}/P_p)$, which is still plausibly below the crust's breaking strain. We conclude that the NS crust is likely strong enough to deform PSR B1828−11 to the extent that it will precess with a period of ∼500 days.

The spin-down strain field suggests that the evolutionary picture of crustal strain might be as follows. Suppose that the star is born relaxed and rapidly spinning. As the star spins down the strain becomes largest first in the upper crust (see Fig. 5). Cracking begins in the upper crust when the yield strain is reached there; however, because relatively little strain energy can be stored in this region of small shear modulus, these small quakes would not be expected to relax the strain that has developed deeper in the crust. When the yield strain is reached deeper, larger (i.e., more energetic) quakes occur there. Eventually an equilibrium is reached in which the strain field is just subcritical throughout the crust. If the Earth is any guide, then numerous small quakes should occur often, while large quakes occur rarely, but release most of the accumulated strain energy. These large

events could excite the precession. We will explore this scenario further in a future publication.

In this picture, one expects that in the upper crust, σ_{ab}^{ref} nearly cancels σ_{ab}^{sd} (so that the sum is below the breaking strain), while near the bottom of the crust, where spin-down strain is lower, the actual strain level $\bar{\sigma}$ is probably greater than $\bar{\sigma}^{sd}$. For example, if the bottom of the crust has not significantly relaxed since the NS's spin was 60 Hz, then the total strain field near the bottom would presumably resemble σ_{ab}^{sd} for spin-down from $\nu_{s,ref} = 60$ Hz.

7. OTHER CANDIDATE PRECESSING PULSARS

So far we have focused our discussion on PSR B1828−11; we now apply our results to other pulsars showing modulations that may be due to precession. Here we discuss the Crab, Vela, PSRs B1642−03, B2217+47, B0959−54, and the possible remnant in SN 1987A. The strength of evidence for precession of these pulsars varies from more or less convincing to marginal; only one of these candidates (PSR B1642−03) shows strongly periodic *and* correlated changes in both pulse shape and phase similar to those observed in PSR B1828−11. In this section we merely summarize all published claims of precession, without attempting to assess their validity.

Our discussion is brief since most these cases have recently been reviewed in depth by Jones & Andersson (2001). Note, however, that our conclusions are often different from Jones & Andersson (2001) because our more accurate value of b is nearly 2 orders of magnitude smaller. Our results are summarized in Table 2.

Before proceeding, we note that two of the precession candidates that we discuss, the Crab and Vela pulsars, suffer glitches in spin rate. Glitches are thought to represent angular momentum transfer to the crust from the interior superfluid as the array of superfluid vortices, usually pinned to nuclei of the crust or magnetic flux tubes in the core, undergoes a sudden expansion (see, e.g., Anderson & Itoh 1975; Link & Epstein 1996; Ruderman, Zhu, & Chen 1998). Even a small amount of vortex pinning is inconsistent with long-period precession (Shaham 1977). For the sake of this discussion, we ignore this objection. We refer the reader to Link & Cutler (2002) for a discussion of how precession could unpin vortices that are initially pinned to the crust.

7.1. *PSR B1642−03*

PSR B1642−03 has $\nu_s = 2.5$ Hz (the same spin rate as PSR B1828−11) and shows a 10^3 day periodicity in pulse shape, with modulation amplitude ≈ 0.05 (Cordes 1993). This period is 120 times shorter than the free-precession period, assuming a relaxed crust. If shear stresses are responsible for PSR B1642−03's ΔI_d, then its reference angular velocity is ~ 27 Hz.

7.2. *PSR B0531+21 (the Crab Pulsar)*

The Crab Pulsar has $P_s = 0.0331$ s; Lyne, Pritchard, & Smith (1988) observed a phase residual with period 20 months, which Jones (1988) interpreted as evidence for precession. Thus, $P_s/P_p = 6.4 \times 10^{-10}$, while for our fiducial NS, we predict $\Delta I_d/I_C \approx 5.4 \times 10^{-9}$ This factor of ~ 8 discrepancy is not large considering the uncertainties in the NS EOS, crust thickness, and the mass and radius of the Crab; we conclude that a 20 month precession period is not in significant disagreement with our theoretical estimate.

This conclusion is contrary to that of Jones & Andersson (2001), who concluded that the discrepancy was a factor ~ 700 instead of ~ 8.

7.3. *PSR 2217+47*

PSR 2217+47 has $P_s = 0.538$ s and was originally thought to have a single-component pulse profile. However, Suleymanova & Shitov (1994) reported the discovery of a weaker second component that varies with a period of ~6–8 yr. Additionally, the braking index of PSR 2217+47 has changed significantly between the original observation epoch (1974–1984) and the subsequent observations (Shabanova 1990). Suleymanova & Shitov (1994) interpret the change in the spin-down rate as evidence for free precession with period at least comparable to the baseline of observations (i.e., $P_p \gtrsim 20$ yr) and attribute the more rapid pulse shape variation to a patchy structure of the emission beam. Taking this interpretation at face value, the reference angular velocity of the crust is $\nu_{s,ref} \lesssim 12$ Hz (compared to the current $\nu_s = 1.86$ Hz) and $\bar{\sigma}_{ave}^{sd} \lesssim 4 \times 10^{-6}$.

7.4. *PSR B0959−54*

D'Alessandro & McCulloch (1997) show that the odd moments of the pulse profile of B0959−54 are negatively

TABLE 2

PRECESSION CANDIDATES: OBSERVATIONS AND INFERENCES

NAME	P_s (s)	$\dot{P}_s$	P_p (days)	$\nu_{s,ref}$ (Hz)	$\nu_{s,ref}^{-1}$ (ms)	CRUSTAL STRAIN $\bar{\sigma}_{pole}^{sd}$	CRUSTAL STRAIN $\bar{\sigma}_{ave}^{sd}$
B1828−11	0.405	6×10^{-14}	511	40	26	2×10^{-3}	5×10^{-5}
B1642−03	0.388	1.78×10^{-15}	1250	25	41	7×10^{-4}	2×10^{-5}
B0833−45 (Vela)	0.0893	1.25×10^{-13}	165	32	31	10^{-3}	3×10^{-5}
B0531+21 (Crab)	0.0334	4.21×10^{-13}	600	10	97	~ 0	~ 0
B2217+47	0.5384	2.77×10^{-15}	>7300	<12	>84	$<2 \times 10^{-4}$	$<4 \times 10^{-6}$
B0959−54	1.437	5.14×10^{-14}	>2500	<33	>30	$<10^{-4}$	$<3 \times 10^{-5}$
SN 1987A	2.14×10^{-3}	...	0.0116	597	1.7	~ 0	~ 0

NOTE.—Summarizes our results for six precession candidates; $\nu_{s,ref}$ is the crust's reference spin value, assuming that crustal rigidity sets the observed precession period. The strain values are the current spin-down strains in the NS crust, i.e., the strains induced when a relaxed star spins down from the reference spin $\nu_{s,ref}$ to the current spin ν_s. For B2217+47 and B0959−54, only lower limits on the precession period are claimed in the literature, yielding lower limits on $\nu_{s,ref}$. For the Crab and SN 1987A, $\nu_{s,ref}$ is less than, or comparable to, ν_s for our fiducial NS model, so there is no evidence of nonzero crustal spin-down strain.

correlated with the variations in the timing residuals. The timing residuals appear quasi-periodic, and so they interpret this observation as evidence for free precession with $P_p \gtrsim 2500$ days (i.e., greater than or equal to the period of the timing residuals). This constraint on P_p implies that the crust's reference angular velocity is $\nu_{s,\mathrm{ref}} \lesssim 33$ Hz (compared to spin frequency $\nu_s = 0.696$ Hz) and $\bar{\sigma}^{\mathrm{sd}}_{\mathrm{ave}} \lesssim 3 \times 10^{-5}$.

7.5. *PSR B0833−45 (the Vela Pulsar)*

The Vela Pulsar has $P_s = 0.089$ s; Deshpande & McCulloch (1996) detected intensity variations with a 165 day period, which they interpreted as possible evidence of precession.

Thus, $P_s/P_p = 6.2 \times 10^{-9}$, while for our fiducial NS, we predict $\Delta I_d/I_C \approx 7 \times 10^{-10}$. The factor of ~9 discrepancy could be accounted for by Vela having a rather small mass and correspondingly large radius (e.g., $M \approx 1.1\ M_\odot$ and $R \approx 18$ km) or by Vela having a crust whose reference angular velocity is $\nu_{s,\mathrm{ref}} \approx 32$ Hz (i.e., 3 times the current spin). The latter would entail an average crustal spin-down strain of $\bar{\sigma}^{\mathrm{sd}}_{\mathrm{ave}} \sim 3 \times 10^{-5}$.

7.6. *Remnant in SN 1987A*

Middleditch et al. (2003) have suggested that there is a precessing pulsar in the remnant of SN 1987A. They present evidence for the existence of a pulsar (now faded from view) with spin period $P_s = 2.14$ ms and evidence for modulation (which they interpret as precession) on a timescale $P_p \sim 10^3$ s, requiring $\Delta I_d/I_C \approx 2 \times 10^{-6}$. Although failure to observe a pulsar in SN 1987A since 1993 brings the existence of a pulsar into question, we apply our results assuming that the pulsar exists. For our fiducial NS parameters, we would expect $\Delta I_d/I_C \approx 1.3 \times 10^{-6}$. The factor of ~1.5 difference is small compared to uncertainties in the NS EOS, mass, etc. We conclude (in contrast to Jones & Andersson 2001) that the 10^3 s precession timescale is quite reasonable, theoretically.

7.7. *Discussion*

Figure 8 summarizes the observational claims of precession presented in this section. In this figure, we plot the observed spin periods of NSs against their claimed precession periods (or lower limits on P_p for PSRs B2217+47 and B0959−54). What limits can we place on the precession periods using the interpretation adopted in this paper, i.e., that the precession is due to a nonspherical shape of the crust? First, $P_p = P_s(I_C/\Delta I_d) = P_s(I_C/b\Delta I_\Omega) \propto \nu^{-2}_{s,\mathrm{ref}}$ (for given ν_s). Dashed lines in Figure 8 show the above relation for $1/\nu_{s,\mathrm{ref}} = 1$ and 20 ms. A pulsar lying below the 1 ms line would have a reference spin frequency faster than 1 kHz. Note that none of the pulsars with claims of precession require uncomfortably large $\nu_{s,\mathrm{ref}}$, i.e., nowhere close to breakup spin of ~1.5 kHz for our fiducial mass and radius. (See Cook, Shapiro, & Teukolsky 1994 for an exhaustive summary of breakup frequencies for various EOSs.)

Second, if the crust of the NS is relaxed at its current spin frequency, then $P_s = 1/\nu_{s,\mathrm{ref}}$ and $P_p \propto \nu^{-3}_{s,\mathrm{ref}}$. This relation is shown by the solid line in Figure 8. Since we presume that the NS had a relaxed crust in the past and has since then spun down, theoretically feasible precession candidates must lie to the right of the solid line. All precession candidates except for the Crab Pulsar satisfy this constraint. The Crab's claimed precession frequency can also be explained in terms of its crustal rigidity, if one assumes that its mass and radius are somewhat different from our fiducial values (e.g., $M = 1.8\ M_\odot$ and $R = 8.0$ km).

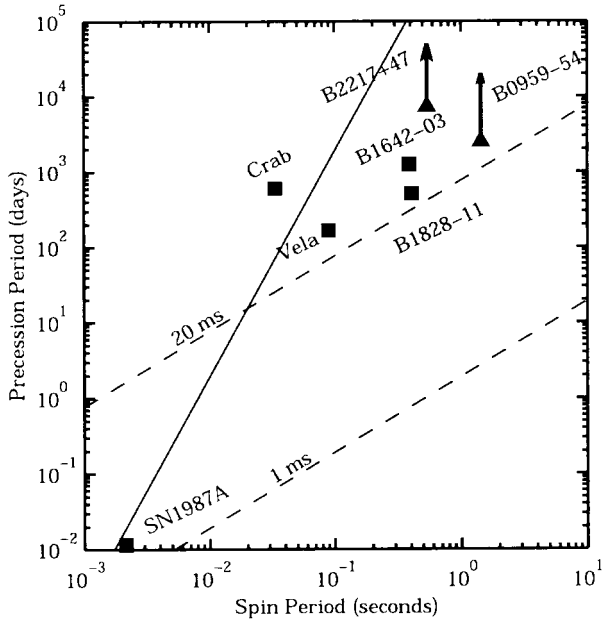

FIG. 8.—Summary of precession candidates and limits on their initial spins. Squares mark spin and precession periods of candidates discussed in § 6, while triangles with arrows indicate lower limits on precession periods for B2217+47 and B0959−54. The dashed lines indicate minimum precession periods of NSs whose crusts last relaxed when they were spinning at 1 ms (*bottom line*) and 20 ms (*top line*). For a given initial spin period, all precessing NSs must lie above the corresponding dashed line. The solid line gives the precession period for NSs with relaxed crusts. NSs that are slowing down should lie to the right of this line.

8. SUMMARY

A relaxed, self-gravitating object with a rigid crust has a portion of its spin-induced bulge that cannot follow changes in the direction of the solid's rotation vector. Such an object can precess, at a frequency that is determined by the material properties of the crust and the strength of gravity, whose relative strengths are determined by the rigidity parameter b. In this paper we showed that a NS's rigidity parameter b is a factor of ~40 times smaller than the estimate of Baym & Pines (1971; see eq. [3]). Using this result, we showed that the precession frequency ν_p for PSR B1828−11 is $\sim 250(511\ \mathrm{days}/P_p)$ times faster than expected for a NS with a relaxed crust, indicating that its crust is significantly strained. The strain would naturally arise from the secular spin-down of the star. Large quakes that partially relax the accumulated strain energy could also excite precession. Applying our results to PSR B1828−11 implies that the average value of spin-down strain in the crust is $\bar{\sigma}^{\mathrm{sd}}_{\mathrm{ave}} \sim 5 \times 10^{-5}$ if the core and crust are effectively decoupled and larger by a factor of $\simeq 100$ if the crust and core are dynamically coupled over a spin period. It is not unreasonable to expect the NS crust to be able to sustain such modest strain values. Applying our model of a relaxed crust to other precession candidates, we found that only SN 1987A and the Crab Pulsar are consistent with the hypothesis of a relaxed crust. The other candidates can be reasonably explained as having strained crusts, although unfortunately this

explanation has no predictive power; the one free parameter (the reference spin) is adjusted to fit the precession timescale.

We conclude here by mentioning one other application of our result for b. Cutler (2002) has shown that for rapidly rotating NSs with relaxed crusts and a strong, interior toroidal magnetic field B_t, the prolate distortion of the star induced by B_t dominates over the oblateness frozen into the crust for $B_t > 3.4 \times 10^{12}$ G $(\nu_s/300\ \mathrm{Hz})^2$. In this case, dissipation tends to drive the magnetic symmetry axis orthogonal to the spin direction, and the NS becomes a potent gravitational wave emitter. Had one used the Baym-Pines value for b, one would have arrived at a substantially larger requirement on the toroidal field (in order for it to dominate over crustal rigidity): $B_t > 1.4 \times 10^{14}$ G $(\nu_s/300\ \mathrm{Hz})^2$.

C. C. was supported in part by NASA grant NAG 5-4093, B. L. was supported in part by NSF grant AST 00-98728, and G. U. was supported by a Lee A. DuBridge postdoctoral fellowship at Caltech.

APPENDIX A

APPROXIMATE b FROM INTEGRAL OF CRUSTAL STRESSES

Our solution for the NS's rigidity parameter b in §§ 3–4 involved calculating the exterior $l = 2$ piece of the gravitational potential $\delta\phi$ for two stars spun up to angular value Ω: (1) a star that is completely fluid and (2) a star with a relaxed, spherical crust that is otherwise identical to the first one. The relative difference in the exterior $\delta\phi$ *is* b. Our result (Table 1) is that $b \sim 2 \times 10^{-7}$, so an accurate calculation of b by the above subtraction method requires solving for $\delta\phi$ to roughly nine decimal places. Here, as an additional check on our work, we estimate b in a way that does not require such high accuracy from our solutions.

UCB derived a identity relating a NS's mass multipole moment Q_{22} to an integral of stresses in the crust. The same calculation can be repeated for the Q_{20} multipole moment. Defining Q_{20} by

$$Q_{20} \equiv \int \delta\rho(r,\ \theta,\ \phi)\, Y_{20}(\theta,\ \phi) dV, \tag{A1}$$

we obtain

$$Q_{20} = -(1-F)^{-1} \int \frac{r^3}{g}\left[\frac{3}{2}(4-\tilde{U})t_{rr} + \frac{1}{3}(6-\tilde{U})t_\Lambda + \sqrt{\frac{3}{2}}\left(8 - 3\tilde{U} + \frac{1}{3}\tilde{U}^2 - \frac{1}{3}r\frac{d\tilde{U}}{dr}\right)t_{r\perp}\right] dr\ , \tag{A2}$$

where $g(r) = Gm(r)/r^2$, $\tilde{U}(r) \equiv 4\pi\rho r^3/m(r)$ [note $\tilde{U}(r) \ll 1$ in the crust], and the stress components of the stress tensor t_{ab} are defined by

$$t_{\mathrm{ab}} = t_{rr}(r)\, Y_{lm}\left(\hat{r}_a\hat{r}_b - \tfrac{1}{2}e_{\mathrm{ab}}\right) + t_{r\perp}(r) f_{\mathrm{ab}} + t_\Lambda(r)\left(\Lambda_{\mathrm{ab}} + \tfrac{1}{2}e_{\mathrm{ab}}\right)\ , \tag{A3}$$

where the tensors e_{ab}, f_{ab}, and Λ_{ab} were defined in equation (59).

The factor $(1-F)^{-1}$ in equation (A2) requires some explanation. UCB derived equation (A2), without that factor, within the *Cowling approximation*, in which the self-gravity of the perturbation is neglected. So $(1-F)^{-1}$ is a correction factor that accounts for the effect of the perturbation's self-gravity. UCB derived an approximate expression for F (UCB, eq. [72]), leading to the estimate that $F \approx 0.2$–0.5, depending on the particular NS model.

We have calculated the right-hand side of equation (A2) for the stresses obtained by solving our case 1, with the source term $(R\Omega/c)^2$ set equal to -1. The result is the residual Q_{20} for a NS whose crust was relaxed at spin $\Omega = c/R$ and that was then spun down to $\nu_s = 0$. We find $Q_{20}|_{\mathrm{residual}} = (1-F)^{-1} 4.24 \times 10^{38}$ g cm^2 for our fiducial 1.4 $M_\odot$ NS, constructed with the AU EOS.

The rigidity parameter b is the residual Q_{20} of the nonrotating NS, divided by the Q_{20} of the rotating model. The latter is given by

$$Q_{20}|_{\mathrm{rotating}} = \frac{5c^2R^3}{4\pi G} z_5|_{r=R}\ , \tag{A4}$$

where $z_5 = \delta\phi/c^2$. For Ω set equal to c/R, we find $Q_{20}|_{\mathrm{rotating}} = 2.8 \times 10^{45}$ g cm^2 for the same fiducial model. Thus, integrating the stresses in the crust yields $b = (1-F)^{-1} 1.5 \times 10^{-7}$ or, for the F in the range 0.2–0.5, $b \approx (1.9\text{–}3.0) \times 10^{-7}$. This is in excellent agreement with the value $b = 2.47 \times 10^{-7}$ in Table 1.

APPENDIX B

ANALYTIC SOLUTION FOR b FOR HOMOGENEOUS SPHERE WITH THIN CRUST

A classic problem solved by Lord Kelvin was the determination of $b \equiv \Delta I_d/\Delta I_\Omega$ for the case of a constant-ρ, constant-μ sphere; the result can be written as $b = (57/10)\mu V/|E_g|$, where V is the star's volume and E_g is its binding energy. (For the derivation, see the classic treatise by Love 1944, p. 259.) In Figure 9 we plot dE_{strain}/dr for this case. We see that the strain

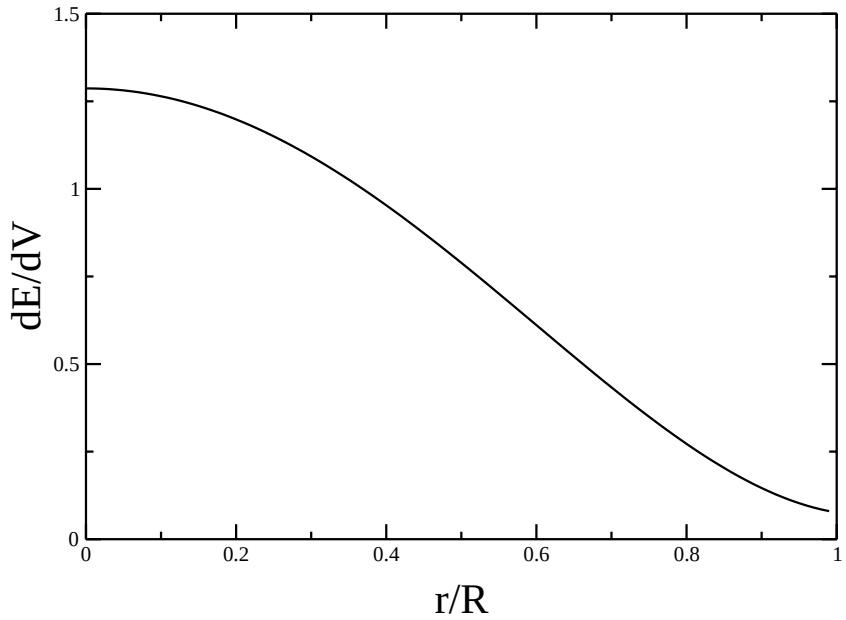

FIG. 9.—Strain energy in a homogenous, elastic sphere, as a function of r. Units are arbitrary.

energy is concentrated toward the center of the star, which already suggests that this model problem will not be a reliable guide for estimating the rigidity of a realistic NS (where all the shear stresses are near the surface).

Here we solve the corresponding problem for a star with a thin crust. That is, we consider a constant-ρ star that consists of two pieces: a fluid interior (where the shear modulus μ is zero) plus a thin crust where μ is constant. Our case is clearly much closer to a realistic NS, where the ratio (crust thickness)/(NS radius) is $\sim 1/20$. Most of the analysis we require has already been carried out by Franco et al. (2000), who solved for the displacements and strain buildup that occur when such a star spins down. Franco et al. (2000) work within the Cowling approximation—i.e., they neglect the gravitational perturbation $\delta\phi$ induced by crustal distortions—so, for convenience, in this appendix we neglect $\delta\phi$ as well. As explained in Appendix A, the Cowling approximation underestimates b by a factor of $\approx 5/3$.

Franco et al. (2000) did not restrict themselves to the case of a *thin* crust, but we do so, for convenience. Rather than repeat their derivation, we simply quote their formulae; e.g., we refer to their 39th numbered equation as equation (F39). Franco et al. define R' and R to be the radii at the bottom and top of the crust, respectively. We define $\Delta R \equiv R - R'$ and neglect terms that are of quadratic or higher order in ΔR. We just highlight the basic steps and refer the reader to Franco et al. (2000) for further details.

We will show that for the thin-crust case, and within the Cowling approximation,

$$b = \frac{12}{11}\frac{\mu V_c}{|E_g|} , \tag{B1}$$

where V_c is the volume of the crust and E_g is still the binding energy of the entire star.

When the star's spin-squared changes by $\delta(\Omega^2)$, the crust undergoes a displacement $\boldsymbol{u}(r, \theta)$, whose radial piece can be shown to have the form $u_r(r, \theta) = f(r)P_2(\theta)$, where P_2 is the second Legendre polynomial and $f(r = R)$ has the form

$$f(R) = \frac{5}{6}R\frac{\delta(\Omega^2)}{v_k^2}\left(1 - b\right) . \tag{B2}$$

Here $v_k^2 \equiv GM/R$ and M is the star's mass. Equation (F31) shows that the Eulerian change in the ($l = 2$ piece of the) gravitational potential exterior to the star is $\propto f(R)$, which makes it clear that the b on the right-hand side of equation (B2) must also equal $\Delta I_d/\Delta I_\Omega$. Expanding equations (F23) and (F24) to linear order in ΔR and substituting into equation (F19), we find

$$f(R) = \tfrac{1}{3}AR^3 - \tfrac{3}{16}BR^{-2} , \tag{B3}$$

$$f'(R) = \tfrac{1}{4}AR^2 + \tfrac{3}{4}BR^{-3} , \tag{B4}$$

$$f'(R - \Delta R) = f'(R) - \Delta R\left[-2AR - \tfrac{3}{4}BR^{-4}\right] , \tag{B5}$$

where $f' \equiv df/dr$ and A and B are coefficients (to be solved for) appearing in the expansion of $f(r)$; see equation (F19). Expanding equation (F38) to linear order in ΔR and comparing with equation (B5), we can solve for B in terms of A:

$$BR^{-3} = -\tfrac{2}{3}AR^2 + \tfrac{2}{5}AR\Delta R . \tag{B6}$$

Plugging equation (B6) into equations (B3) and (B4) yields

$$f(R) = \tfrac{11}{24} AR^3 - \tfrac{3}{40} AR^2 \Delta R \,, \tag{B7}$$

$$f'(R) = -\tfrac{1}{6} AR^2 + \tfrac{3}{10} AR \Delta R \,, \tag{B8}$$

and plugging equations (B7) and (B8) into equation (F33) yields

$$f(R) = \frac{5}{6} R \frac{\delta(\Omega^2)}{v_k^2} \left(1 - \frac{60}{11} \frac{\Delta R}{R} \frac{c_t^2}{v_k^2} \right) , \tag{B9}$$

where $v_k^2 \equiv \mu/\rho$. The second term in parentheses on the right-hand side of equation (B9) is b and can be reexpressed as

$$b = \tfrac{12}{11} \mu V_c / |E_g| \,. \tag{B10}$$

Note that the coefficient 12/11 in equation (B10) is smaller than the 57/11 in the Baym-Pines estimate, equation (3), by $209/40 \approx 5.23$. So from our uniform, thin-crust model, we see that the Baym-Pines expression significantly overestimates the rigidity of a NS.

If we were to simply replace the 57/11 in the Baym-Pines estimate by 12/11, we would *still* overestimate the rigidity of a realistic NS by a factor of $\sim$8. To understand this factor, it is instructive to evaluate $Q_{20}|_{\rm residual}$ for the uniform, thin-crust case using our integral expression equation (A2) and compare with the realistic case. For the uniform, thin-crust case, $\tilde{U} = 3$, and using equation (76) in UCB, we find that the correction factor $(1 - F)^{-1}$ is exactly 5/2. The results in Franco et al. (2000) and a few pages of algebra suffice to show that, to leading order in ΔR,

$$\sigma_{rr} = \frac{10}{33} \sqrt{\frac{4\pi}{5}} \frac{R^3 \Omega^2}{GM} \,, \qquad \sigma_\Lambda = \frac{10}{33} \sqrt{\frac{4\pi}{5}} \frac{R^3 \Omega^2}{GM} \,, \qquad \sigma_{r\perp} = 0 \,, \tag{B11}$$

for the case of star spun down from Ω to zero angular velocity. Also, for a uniform star rotating at angular velocity Ω,

$$Q_{20} = \frac{5}{6} \sqrt{\frac{4\pi}{5}} \rho R^5 \frac{R^3 \Omega^2}{GM} \,. \tag{B12}$$

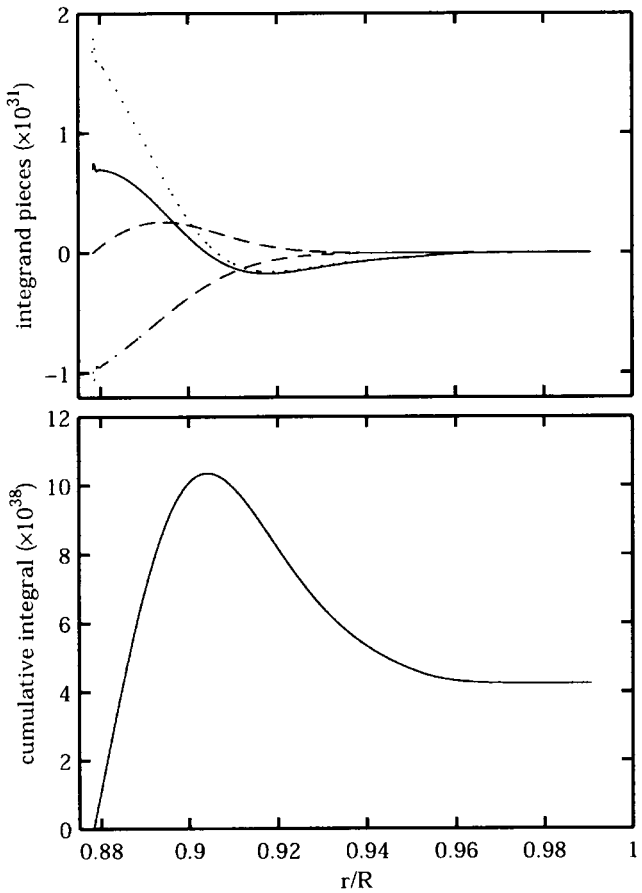

FIG. 10.—*Top*: Pieces of the integrand of eq. (A2) proportional to t_{rr} (*dotted line*), $t_{r\perp}$ (*dashed line*), and t_Λ (*dot-dashed line*), computed for model AU. *Bottom*: Cumulative integral.

Using these results and equation (A2), we find that the term $\propto\sigma_{rr}$ in equation (A2) contributes $-\frac{1}{2}(12/11)\mu V_c/|E_g|$ to b, while the term $\propto\sigma_\Lambda$ contributes $(3/2)(12/11)\mu V_c/|E_g|$.

Comparing these intermediate results to those for the realistic NS case (with compressible matter and a steep density gradient), we see that in the realistic case, there is much more cancellation within the integral for Q_{20}. As shown in Figure 10, in the realistic case both σ_{rr} and σ_Λ switch signs at different depths inside the crust (so that the contributions to b from different layers tend to cancel each other, unlike in the uniform, thin-crust case). Also, the σ_{rr} and σ_Λ contributions are clearly much closer in magnitude (although still of opposite sign) in the realistic case and so cancel each other much more nearly.

REFERENCES

Abney, M., Epstein, R. I., & Olinto, A. V. 1996, ApJ, 466, L91
Alpar, A., & Pines, D. 1985, Nature, 314, 334
Anderson, P. W., & Itoh, N. 1975, Nature, 256, 25
Baym, G., & Pines, D. 1971, Ann. Phys., 66, 816
Cook, G. B., Shapiro, S. L., & Teukolsky, S. A. 1994, ApJ, 424, 823
Cordes, J. M. 1993, in ASP Conf. Ser. 36, Planets around Pulsars, ed. J. A. Phillips, S. E. Thorsett, & S. R. Kulkarni (San Francisco: ASP), 43
Cutler, C. 2002, Phys. Rev. D, 66, 08025
D'Alessandro, F., & McCulloch, P. M. 1997, MNRAS, 292, 879
Deshpande, A. A., & McCulloch, P. M. 1996, in IAU Colloq. 150, Pulsars: Problems and Progress, ed. S. Johnston, M. A. Walker, & M. Bailes (ASP Conf. Ser. 105; San Francisco: ASP), 101
Franco, L. M., Link, B., & Epstein, R. I. 2000, ApJ, 543, 987
Jones, D. I. 2000, Ph.D. thesis, Univ. Wales, Cardiff
Jones, D. I., & Andersson, N. 2001, MNRAS, 324, 811
Jones, P. B. 1988, MNRAS, 235, 545
Kaminker, A. D., Pethick, C. J., Potekhin, A. Y., Thorsson, V., & Yakovlev, D. G. 1999, A&A, 343, 1009
Link, B., & Cutler, C. 2002, MNRAS, 336, 211
Link, B., & Epstein, R. I. 1996, ApJ, 457, 844
———. 2001, ApJ, 556, 392
Lorenz, C. P., Ravenhall, D. G., & Pethick, C. J. 1993, Phys. Rev. Lett., 70, 379
Love, A. E. H. 1944, A Treatise on the Mathematical Theory of Elasticity (4th ed.; New York: Dover)
Lyne, A. G., Pritchard, R. S., & Smith, F. G. 1988, MNRAS, 233, 667
McDermott, P. N., van Horn, H. M., & Hansen, C. J. 1988, ApJ, 325, 725
Mendell, G. 1998, MNRAS, 296, 903
Mestel, L., Nittman, J., Wood, W. P., & Wright, G. A. E. 1981, MNRAS, 195, 979
Mestel, L., & Takhar, H. S. 1972, MNRAS, 156, 419
Middleditch, J., et al. 2003, PASP, in press (astro-ph/0010044)
Munk, W. H., & MacDonald, G. J. F. 1960, The Rotation of the Earth (Cambridge: Cambridge Univ. Press)
Negele, J. W., & Vautherin, D. 1973, Nucl. Phys. A, 207, 298
Nittmann, J., & Wood, W. P. 1981, MNRAS, 196, 491
Oyamatsu, K. 1993, Nucl. Phys. A, 561, 431
Pines, D., & Shaham, J. 1972a, Nature Phys. Sci., 235, 43
———. 1972b, Phys. Earth Planet. Inter., 6, 103
Press, W. H., Teukolsky, S. A., Vetterling, W. T., & Flannery, B. P. 1992, Numerical Recipes in C (Cambridge: Cambridge Univ. Press)
Ruderman, M., Zhu, T., & Chen, K. 1998, ApJ, 492, 267
Shabanova, T. V. 1990, AZh, 67, 536
Shaham, J. 1977, ApJ, 214, 251
———. 1986, ApJ, 310, 780
Spitzer, L., Jr. 1958, in IAU Symp. 6, Electromagnetic Phenomena in Cosmical Physics, ed. B. Lehnert (Cambridge: Cambridge Univ. Press), 169
Strohmayer, T. E., van Horn, H. M., Ogata, S., Iyetomi, H., & Ichimaru, S. 1991, ApJ, 375, 679
Stairs, I. H., Lyne, A. G., & Shemar, S. L. 2000, Nature, 406, 484
Suleymanova, S. A., & Shitov, Y. P. 1994, ApJ, 422, L17
Ushomirsky, G., Cutler, C., & Bildsten, L. 2000, MNRAS, 319, 902 (UCB)
Wasserman, I. 2003, MNRAS, in press
Wiringa, R. B., Fiks, V., & Fabrocini, A. 1988, Phys. Rev. C, 38, 1010